Front. Phys. 11(6), 117405 (2016)
DOI 10.1007/s11467-016-0577-2

REVIEW ARTICLE

A brief review of co-doping

Jingzhao Zhang, Kinfai Tse, Manhoi Wong, Yiou Zhang, Junyi Zhu†

Department of Physics, the Chinese University of Hong Kong, Shatin, N.T., Hong Kong 999077, China
Corresponding author. E-mail: †jyzhu@phy.cuhk.edu.hk
Received February 2, 2016; accepted March 10, 2016

Dopants and defects are important in semiconductor and magnetic devices. Strategies for controlling doping and defects have been the focus of semiconductor physics research during the past decades and remain critical even today. Co-doping is a promising strategy that can be used for effectively tuning the dopant populations, electronic properties, and magnetic properties. It can enhance the solubility of dopants and improve the stability of desired defects. During the past 20 years, significant experimental and theoretical efforts have been devoted to studying the characteristics of co-doping. In this article, we first review the historical development of co-doping. Then, we review a variety of research performed on co-doping, based on the compensating nature of co-dopants. Finally, we review the effects of contamination and surfactants that can explain the general mechanisms of co-doping.

Keywords co-doping, fully compensated, partially compensated, non-compensated, unintentional doping, surfactant

PACS numbers 74.62.Dh, 74.72.Ek, 74.72.Gh, 61.72.-y

Contents

1 Introduction

Doping is crucial for determining physical properties and applications of various materials, especially semiconductors. This notion has been confirmed by tremendously successful applications in semiconductor industry. Minor quantities of impurities determine the carrier concentrations and electrical conductivities of the materials. Fundamentally, a good dopant should achieve an ideal solubility in its host material and should exhibit a shallow defect level. However, there exist some fundamental doping bottlenecks, which strongly affect the device performance. In the case of wide band-gap materials, the problems are severe. For example, *n*-type doping was found to be difficult for high conduction-band minimum (CBM) energy; on the other hand, *p*-type doping was found to be difficult for low valence-band maximum (VBM) energy [1]. As a result, bipolar doping problems exist in many wide band-gap semiconductors, where either *n*-type or *p*-type dopants can be doped, but not both [2]. Therefore, a feasible solution is to simultaneously incorporate certain amounts of *p*-type and *n*-type dopants, for lowering their formation energy, which is also the fundamental principle of compensated co-doping.

Co-doping has been proposed for solving the problems of bipolar doping and compensation in semicon-

ductors. In general, co-doping can be efficient for increasing the dopant solubility, increasing the activation rate by lowering the ionization energy of acceptors and donors, and increasing the carrier mobility [3]. Enhanced dopant incorporation is especially significant under non-equilibrium growth conditions owing to the introduction of new chemical species as co-dopants [2]. For example, without any co-dopants, the maximum hole concentration in Mg doped GaN is around 10^{17}cm^{-3} [4]. However, such concentration can be raised for an order of magnitude when Mg and O are co-doped [5, 6].

This paper is organized as follows. First, the history of co-doping is briefly reviewed. Next, we describe the methods of fully compensated co-doping, co-doping with partial compensation, co-doping without compensation, and unintentional co-doping. Then, we review surface effects and effects of defect complexes. Finally, we list our conclusions and provide an outlook.

2 Historical roadmap of co-doping

Although this paper focuses on co-doping, it is essential to first review the early history of doping. In 1930, Gudden noticed that conductivity of semiconductors was almost entirely due to the presence of minute quantities of impurities [7, 8]. In 1931, Wilson was the first to apply the quantum mechanical formalism to semiconductors [9]. Later, the idea of p-type and n-type doping was put forward in a few pioneering works on rectifiers, based on copper oxide [10] and selenium (Se) [11, 12]. The first model of a p–n junction was contributed by Davydov in 1938 [8, 13], who also explained the importance of minority carriers. As for a real experimental realization, in 1944, Woodyard was the first to develop a nonlinear circuit device using germanium (Ge) [14]. Woodyard also introduced the concept of "doping" [14]. Small controlled amounts of phosphorus (P), arsenic (As), or antimony (Sb) were incorporated into pure Ge to improve the electrical characteristics of circuit junctions [14]. In 1949, Shockley theoretically proposed a major innovation, namely, the "junction transistor" [15]. He posited that this novel device was superior to the point-contact type device [16]. However, manufacturing of junction transistors was plagued by a difficult problem: the device required a thin-spaced, sandwiched layer of two p–n junctions, joined back-to-back [16]. A solution was found in 1950, when Sparks and Teal, working at Bell Labs, fabricated a "grown junction transistor" using a technique known as "double doping" [17, 18]. The first step in the proposed double doping process utilized molten n-type Ge; by adding a small amount of gallium (Ga), the molten Ge was transformed into p-type Ge. Then, moments later, a small pill of Sb was added to convert the p-type back to the n-type [16]. In this process, two types of dopants were introduced simultaneously. In a more general sense, a p–n junction can be considered as "co-doping" of p-type and n-type dopants into different regions of a semiconductor material.

The early history of co-doping can be traced back to the early 1950s. In 1952, Fuller studied the diffusion of donors and acceptors in Ge [19]. In 1953, he studied the diffusion and solubility of lithium (Li) in Ge- and silicon-based (Si-based) p–n junctions, and determined that Li acts as a strong donor [20]. Later, Reiss *et al.* studied the ionization effects of donors and acceptors on the electronic properties of semiconductors [21]. The solubility of Li in boron-doped (B-doped) Si was studied [22]. A mechanism for describing inter-defect interactions in Ge and Si was also proposed [23]. In 1956, Kröger and Vink proposed that the impurities with opposite effective charges tend to increase each other's concentration [24, 25]. Later, the effects of ion pairing in Si [26] and the solubility of Li in Ge in the presence of Ga and zinc (Zn) [27] were studied too. It was found that co-doping can lead to increased conductivity owing to a number of factors [28]: (i) an enhanced equilibrium solubility, (ii) lower ionization energy, (iii) change in the carrier mobility. In 1960, Shockley and Moll reached a similar conclusion, stating that the solubility of a charged impurity in a semiconductor depends on the Fermi level [29].

Despite these fundamental works on co-doping, to the best of our knowledge, "co-dope" related words (such as "co-doping" and "co-doped") were introduced in 1963 [30] and were later used in other articles. The research at the time aimed to determine the mechanisms compensating for unintentional introduction of multiple dopants, and chemical mechanisms of growing and doping in materials such as alkaline earth halides (e.g., CaF_2, BaF_2, etc.) doped with rare earths or uranium (U), for potential use in optically pumped lasers [30, 31]. In addition, optical energy transfer was investigated for chromium (Cr) and neodymium (Nd) doubly doped into $Yt_3Al_5O_{12}$ (YAG) [32] and other Cr-doped materials [33].

In the 1960s, a general descriptor of "co-doping" was mainly applied to describe the studies of absorption and luminescence properties. For example, these words were used to describe interactions between Eu^{3+} and other rare earth elements in Y_2O_3 [34], the effect of Pr^{3+} fluorescence on LaF_3 owing to the presence of other rare earth co-dopants [35], the characteristics of Nd^{3+} and Yb^{3+} co-doped LaF_3 [36], and the characteristics of Nd^{3+} and Ce^{3+} co-doped $LaCl_3$ [37]. Rare earth-doped glass [38] was co-doped with UO_2^{2+}, Fe^{2+} [41], for use in saturable-absorber giant-pulse lasers [42]. The optical spectra of CdF_2 single crystals co-doped with compounds such as YbF_3 and NaF were investigated as well in 1967 [43]. In 1969, the influence of an additional im-

purity ion, Ce^{3+}, on the fluorescence of Gd^{3+} in SrF_2 was examined [44]. In addition, the protecting method of S and Mg co-doping into an electrode $NiCl_2$ was reported for applications to batteries [45]. Other co-doping effects related to absorption or fluorescence of Si [46], $SrTiO_3$ and TiO_2 [47, 48], GaP [49, 50], ZnSe [51, 52], ZnS [53], and CdS [54] were also reported. In a different line of work, solution and diffusion of impurities in heavily doped semiconductors were addressed, as well as interactions among pairs of impurity ions. For example, an impurity interaction mechanism for P and Ga [55] and reactions of group III acceptors with O [56] in Si were investigated. Studies on vibrational modes of Li-O, Li-B in Si [57], Li-P [58] in Ge, were performed along with studies on cooperative diffusion in p–n–p structures [59]. The distribution and precipitation of gold (Au) in heavily phosphorus-doped (P-doped) Si [60-62] was revealed, and some experimental results of these studies [61] were consistent with the Reiss theory. In addition, ion pairing between Li and acceptors was discovered in GaSb [63] and GaAs [64].

In the 1970s, studies of rare earth-related co-doped laser rob materials (such as YAG) continued in the field of lasers [65–69]. Investigations of infrared quantum counters [70] and infra red (IR) up-converting phosphors [71] were also performed, addressing the effects of co-doping of certain materials (such as CaF_2 and SrF_2) with rare earth elements or iron (Fe) [72–74].

In the 1970s, compared with the field of lasers, the word "co-dope" was not widely used in the field of traditional semiconductors. However, researches related to the effects of co-doping were widely reported. For example, the phenomena of Li-Li-O luminescence [75], Zn-O pairs [76] in GaP, defect pairs in ZnSe [77], CdS, and CdTe [78], were studied. The focus of the co-doping research at that time shifted toward wide-gap semiconductors. Researchers mainly focused on studying the effects of co-doping on optical properties and on studying the mechanisms of dopant pair interactions in these wide band-gap materials.

In the 1980s, in the application of a glass laser hosted by a silica (SiO_2) glass, co-doping was used to achieve ideal fluorescence properties for SiO_2 glasses [79–81] and SiO_2 optical fibers [82]. In addition, co-doping positively affected the crystal growth of GaAs single crystals [83]. Moreover, effects of co-doping were established for InP [84–88], and this method was applied for fabricating related devices [89]. In the 1990s, studies on contamination-related effects of defect complexes and diffusion, such as the studies of Fe, copper (Cu), or hydrogen (H) in Si [90–94] or wide band-gap materials [95, 96], had attracted significant attention. More importantly, the tendency to overcome the doping bottle neck of wide band-gap materials [2, 97–100], such as nitrides and oxides, using co-doping, has become increasingly prominent. In this article, we review several works performed in this direction. Thus far, doping of wide band-gap semiconductor materials, such as GaN, ZnO, and TiO_2, remains a significant challenge.

3 Fully compensated co-doping

Fully compensated co-doping, or fully passivated co-doping, refers to the formation of overall electrically neutral neighboring n-type and p-type defects. By using compensated dopants, the dopant solubility can be enhanced owing to the charge transfer between the donor and acceptor, and the Coulomb interaction between the charged defects [98]. Moreover, as discussed above, the Fermi energy is shifted towards VBM(CBM) with increasing the concentration of a $p(n)$-type dopant, so that the formation energy of $n(p)$-type defects is lowered proportionally. Self-compensation, i.e., formation of compensating intrinsic defects such as vacancies, antisites, and interstitials in an appropriate charge state, is thus driven thermodynamically. By applying fully compensated co-doping, the extent of compensation by undesirable intrinsic defects can be lowered, because the charge transfer between neighboring donors and acceptors largely restores the Fermi level. Although fully compensated co-doping is not effective in directly enhancing the dopant concentration, it is valuable in band structure engineering for effectively tuning the band edge and band-gap. Moreover, subsequent annealing of the defects of co-dopants, performed after co-doping, can effectively enhance the population of desired dopants. A significant body of research has been performed in this field. Due to the length limitation on this article, below we will focus on reviewing two interesting problems.

3.1 Band-gap engineering of TiO_2

TiO_2 has been actively considered as a photocatalyst for H_2 production by photo-electrochemical water splitting and other pollutant degradations. For a redox reaction to be energetically favorable, the CBM (VBM) must be higher (lower) than the redox potential of the corresponding reduction (oxidation) reaction [101]. For undoped TiO_2, the valence band (VB) and conduction band (CB) consist of mainly O $2p$ states and titanium (Ti) $3d$ states, respectively, and are 1.6 eV lower and 0.3–0.4 eV higher than the corresponding redox potential for water splitting [101]. However, this 3.2 eV band-gap of undoped TiO_2 completely prevents absorption in the visible spectrum, resulting in a low catalytic efficiency under a visible light illumination [101–103]. A desirable material should have a band-gap narrower than 2.0 eV,

with the band-edges matching the redox potentials [104]. Attempts have been made to improve efficiency by doping or co-doping with transition metal cations or anions for suitably narrowing the band-gap; however, the use of single dopant results in the presence of charged defects, which act as recombination centers and reduce the carrier lifetime, limiting the material's catalytic efficiency [101, 105].

Different strategies for co-doping of TiO_2 have been proposed. By using first-principles calculations, Gai *et al.* proposed a transition metal-anion co-doping strategy using (V/Nb + N) and (Cr/Mo + C) [101]. Long *et al.* studied the passivated dopant pair (C + W/Re/Os) [106]. The co-doped band structure largely follows the mono-doped case, where nitrogen (N) and C anion substitution can lead to the defect band extending to ∼0.5 eV and 0.8–1.1 eV above the VBM, respectively [101, 106]. The CBM position can be maintained for (Mo + C) dopant pairs [101], suitable for water splitting. For the case of (Nb + N) co-doping, Breault *et al.* demonstrated experimentally a 7-fold increase in the rate of photocatalytic decomposition [107]. For (Mo + C) co-doped TiO_2, Dong *et al.* [108] and Zhang *et al.* [102] observed photocurrents [102] and improved catalytic activity [102, 108], in agreement with the elimination of recombination centers by co-doping elements. However, the band-gap was narrowed only to 3.0 eV [102], not as significant as the theoretical prediction [101]. The deviation was attributed to the low concentration of dopant and N_2 adsorption on the surface [102]. (W + C) co-doped TiO_2 synthesized by Neville *et al.* [109] and by Xiao *et al.* [110], and (N + V) co-doped TiO_2 synthesized by Xu *et al.* [111], also exhibited similar red-shifts of the absorption edge. Improving the catalytic activity by (W + C) co-doping is inconclusive, and Xiao *et al.* demonstrated an increased photocatalytic activity with (W + C) co-doping compared to the undoped case [110], while the opposite was observed by Neville *et al.* [109]. The presence of elemental C and Ti-O-C bonding [102, 108] suggests that doped C mostly remains in its elemental phase, with only a relatively minor amount incorporated into TiO_2 in the form of interstitial or anion substitutional defects. All of these detrimental defects may affect the reaction mechanism [108]. This also demonstrates the difficulty associated with doping of C into TiO_2. Ma *et al.* showed that by utilizing the ease of incorporation of a transition-metal dopant, the formation energy of (2Nb/2Ta+C) can be significantly reduced, particularly in the O-rich limit [112].

Other than the transition metal-anion co-doping scheme discussed above, Long *et al.* [103, 113, 114] proposed co-doping of transition metal pairs with a complimentary valence for avoiding an isolated defect band, which exhibits inferior oxidative power and mobility [115]. Charge-compensated dopant pairs of (Mo + Zn/Cd), (Ta + Ga/In) [103] and (Mo/W + Mg/Ca) [114] were modeled by the formation of cation substitutional defects on the neighboring Ti sites. In the case of (Ta + Ga/In), fully compensated co-doping eliminates the intermediate defect band of Ti 3*d* that originates from local distortion [103]. In the case of (Mo + Zn/Cd/Mg/Ca), a defect band with mainly molybdenum (Mo) 4*d* component was reported to form, which is ∼0.4 eV below the CB [103, 114]. The Zn 3*d* band is ∼0.1 eV above the VB [103]. Improved catalytic activity is expected owing to the increased density of states compared with the isolated defect band for transition, and owing to the elimination of recombination centers.

In summary, these studies suggest that fully compensated co-doping of TiO_2 can only partially improve the efficiency owing to the limited solubility of dopants, detrimental *n*-type dopants that significantly lower the CBM, detrimental gap states induced by the dopants, unwanted surface adsorption, and detrimental secondary phases of dopants formed in the crystal. Although it is possible to increase the VBM, the intrinsic challenge of co-doping associated with TiO_2 band engineering is that we should not significantly lower the CBM simultaneously. This limitation strongly constrains the choice of candidate co-doping pairs.

3.2 P-type doping of GaN

Co-doping of *p*-type GaN by Mg and H pairs is one of the most enchanting examples of fully compensated co-doping. Mg-doped *p*-type GaN crystals grown by using high-temperature techniques inevitably form N vacancies (V_N), which are triple donors. Further increase in the partial pressure of an Mg precursor does not increase *p*-type conductivity, because charge compensation effects owing to the presence of N vacancies are energetically favorable [116]. However, because H is inevitably present in organometallic vapor phase epitaxy (OMVPE), this unintentionally co-doped H forms complexes of Mg and H defects with the formation energy lower than that of V_N [116]. As shown in Fig. 1, this compensating technique yields ∼3 orders of magnitude enhancement in the concentration of Mg_{Ga} [116]. The desired *p*-type conductivity can be activated by low-energy electron beam irradiation or thermal annealing [117]. A detailed explanation on the removal of compensating H will be provided in the section on unintentional co-doping below.

Fully compensated co-doping for enhancing the population of desired defects is one of the major advantages of co-doping, which has been widely applied in many semiconductor materials. Such techniques are often combined with post annealing techniques for removal of H from the defect complexes. Species with low diffusion barriers are

often good candidates to serve as co-doping agents, because in general they can be easily removed. The full discussion on H-related defect complexes is far beyond the scope of this article. Here, we will focus on describing only the fundamental principles.

4 Partially compensated co-doping

Similar to fully compensated co-doping, partially compensated co-doping utilizes the charge compensation effect and Coulomb attraction between *n*-type and *p*-type dopants for enhancing the solubility of the dopants. However, different amounts of donors and acceptors are introduced into the system in the case of partially compensated co-doping (e.g., co-doping of a single donor with a double acceptor), making it possible to create partially occupied intermediate bands in the band-gap of the host system. Such scheme has been also referred to as non-compensated *n*–*p* co-doping [118-121]. Nevertheless, to distinguish this co-doping from non-compensated co-doping, in which the stabilization of co-doping pairs is not related to the formation of *n*–*p* pairs, it is perhaps better to refer to it as to partially compensated co-doping, emphasizing the nature of partial compensation in this co-doping scheme. Apart from the enhanced solubility, the presence of intermediate bands reduces the band-gap and enhances optical absorption. Therefore, partially compensated co-doping applies to the doping and band-gap engineering of large band-gap materials, as well as to the design of intermediate-band solar cell materials. This scheme is probably the most widely applied co-doping method among the existing co-doping techniques. Applications in different material systems are described in details in the following sections.

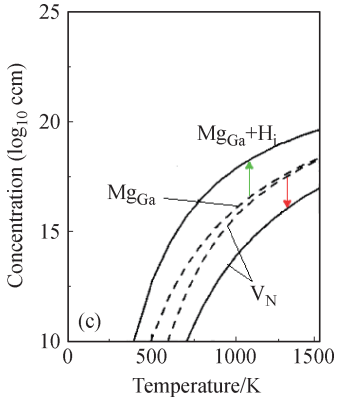

Fig. 1 Equilibrium concentration of Mg_{Ga} substitutional and N vacancy defects with (*solid lines*) and without compensating H (*dotted lines*), arrows indicates the corresponding enhancement of Mg_{Ga} (*green*) and suppression of V_N (*red*). Reproduced from Ref. [116].

4.1 TiO_2

As discussed in the previous sections, TiO_2 is one of the most promising photo-catalyst materials, yet its efficiency is largely limited by its large intrinsic band-gap [100, 122–124]. In addition, dopant solubility in TiO_2 is usually low, particularly for *p*-type dopants, owing to the low VB and spontaneous formation of native defects [100]. While fully compensated co-doping could enhance dopant concentration and reduce the band-gap, the effect of the band-gap narrowing is not very significant, and the created occupied states inside the band-gap are usually localized and might become non-radioactive recombination centers. To overcome these difficulties, Zhu *et al.* proposed partially compensated co-doping of TiO_2 [118]. First-principles calculations showed that chromium-N (Cr-N) co-doping (a net *p*-type) enhanced the incorporation of N into O sites in anatase TiO_2, both thermodynamically and kinetically [118]. Moreover, apart from a comparable band-gap reduction compared with compensated Cr-C or V-N co-doping, strong hybridization of partially compensated *n*–*p* pairs created extended intermediate bands that were broader than the localized impurity levels [118]. Experimental results also confirmed the band-gap reduction and enhancement of photo-activity by co-doping Cr and N into TiO_2 [118]. Besides the photo-catalyst application, formation of intermediate bands is also desirable for design of solar-cell materials [125], which will be described below.

Following this finding, additional theoretical and experimental works have been conducted to study the effect of Cr-N co-doping into TiO_2. Kurtoglu *et al.* found that photo-activity of Cr-N co-doped TiO_2 under ultraviolet (UV) irradiation increased 10-fold compared with mono-doped samples. In addition, their first-principles calculations further demonstrated that negatively charged defect centers of Cr_{Ti}^{-}-N_O^{-} may help to reduce the concentration of trivalent Ti and increase photo-activity [126]. On the other hand, Li *et al.* reported enhanced photo-degradation of methyl orange under visible light for Cr-doped or Cr-N co-doped TiO_2, compared with undoped or N-doped cases; yet, reduced photo-activity under UV irradiation was observed in all doped samples [127]. Experiments by Chiodi *et al.* showed that Cr-N co-doping into nano-clustered TiO_2 thin films occurs on the substitutional sites and delocalized states are created inside the band-gap [128], consistent with earlier theoretical predictions [118]. In addition, experimental observations by Jaćimović *et al.* showed that the effect of Cr-N co-doping largely depends on the growth condition, implying the critical role of structural defects in the doping process [129]. Wang *et al.* confirmed that co-doped Cr and N should both be substitutionally doped into TiO_2, and the band-gap is narrowed to less than 2 eV, mainly owing to lifting of the VBM [130]. Cheney *et al.* iden-

tified the nature of intermediate bands as Cr $3d^3$ levels, and suggested that the observed delocalized N-derived $2p$ states near the CBM could provide the required carrier mobility for photo-catalyst or photovoltaic applications [131]. Lu *et al.* showed that a small amount of N in Cr-doped TiO_2 reduces the concentration of Cr^{6+} and suppresses electron-hole recombination [132]. Besides photo-catalyst materials, Cr-N co-doped TiO_2 was also used as an anode for Li ion rechargeable batteries [133]. Enhanced electrical conductivity was measured following Cr-N co-doping, resulting in an improved performance compared with N mono-doped samples [133].

Other than Cr-N co-doping, some research has focused on the effects of other partially compensated co-doping pairs in TiO_2. Khan *et al.* performed density functional theory (DFT) calculations and found that Mo-N co-doping could reduce the band-gap to 1.5 eV, enhancing the absorption of visible light [134]. Experiments conducted by Zhang *et al.* confirmed the enhanced absorption of visible light, as well as an improved separation of electron-hole pairs [135]. Due to the lifting of the CB edge following the doping with Mo, the optimal concentration of Mo was found to be ~1% [135, 136].

4.2 Intermediate-band solar cell materials

To improve the quantum efficiency of a single junction, Luque and Martí proposed intermediate-band solar cell (IBSC) materials [125], in which a half-full impurity band is introduced into the semiconductor band-gap, as shown in Fig. 2. Owing to the additional optical transition from the VB to the CB via the intermediate band, lower-energy photons in the solar spectrum can be utilized to generate a photocurrent [119, 125]. As a consequence, the maximal efficiency of this device can reach 63.2%, much higher than the Shockley–Queissier limit for a single band-gap semiconductor [137]. The major challenge here is the controlled creation of intermediate bands inside the intrinsic band-gap of the candidate system [119]. Because partially filled delocalized states can be created inside the band-gap by partially compensated co-doping, and because the location of these intermediate bands can be tuned by choosing different co-doping pairs, partially compensated co-doping in large band-gap semiconductors becomes a promising strategy for designing IBSC materials [118]. A theoretical model, based on partially compensated co-doping of TiO_2, predicted that the optimal efficiency can reach 52.7%, and can be even higher (56.7%) if current is allowed to be extracted from the intermediate bands [119].

Although partially compensated co-doping is a promising strategy for designing IBSC materials, the co-doping scheme unavoidably introduces many impurity atoms into the host system, increasing the probability of non-radioactive recombination of photo-generated electron-hole pairs. To avoid introducing too many impurity atoms, a new strategy based on single-element partially compensated co-doping was proposed [120, 121]. By performing first-principles calculations for $CuAlSe_2$, Li *et al.* predicted that P can be substitution ally doped into adjacent aluminum (Al) sites and Se sites, thus behaving simultaneously as a double-donor and single acceptor [120]. The created half-full intermediate band significantly increases the optical absorption coefficient [120]. In addition, Han *et al.* predicted that doping group V elements (P, As, or Sb) into $CuGaS_2$ can create partially filled intermediate bands in the intrinsic band-gap, which is potentially promising for photovoltaic applications [121].

4.3 GaN

Group III-nitride semiconductors have attracted significant attention for applications in opto-electronic devices owing to their tunable and direct band-gap, and obtaining low-resistivity p-type GaN is one of the critical issues in the utilization of GaN-based opto-electronic devices [3, 5, 28, 139, 140]. Similar to TiO_2, there is a natural doping limit for GaN, owing to its low-lying VB [100]. Attempts have been made to improve hole concentrations and conductivities of p-type GaN. In 2001, Katayama-Yoshida *et al.* proposed that formation of the acceptor-donor-acceptor (ADA) complex by co-doping donors and acceptors in GaN would increase the p-type conductivity [3, 139]. Although a single acceptor and single donor are used in this co-doping model, the unbalanced dopant numbers guarantees the partially compensated nature. The theoretical predictions made by these authors were consistent with the experimental observations of an enhanced hole concentration in Be-O co-doping [141], Mg-

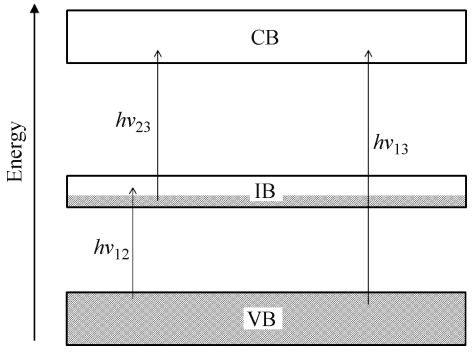

Fig. 2 Band diagram of the IBSC material, in which a half-filled intermediate band (IB) is introduced between the valence band (VB) and conduction band (CB). Optical transition between bands is indicated on the figure. Reproduced from Ref. [138].

O co-doping [5, 6], and Mg-Si co-doping [142]. The experimental observations and the ADA complex model have been reviewed in details by Korotkov *et al.* [28]. Later it has been also proposed that charge redistribution near the Mg_{Ga}-Si_{Ga} complex could enhance the piezoelectric field in GaN, thus splitting the tops of VBs [140]. Such splitting results in the upshift of the VBM and might lower the hole activation energy in GaN, leading to an increased hole concentration [140].

Because GaN is chemically stable even under harsh conditions, and band edges are located to enable water splitting under UV irradiation, this device is also considered to be a promising photo-catalyst [143, 144]. To improve the absorption of visible light by this wide band-gap semiconductor, Pan *et al.* proposed partially compensated Cr-O co-doping in GaN [144]. Their first-principles calculations showed that incorporation of cations can be enhanced by co-doping with anions, owing to the reduced formation energy of the partially compensated complex, and the Fermi level can be shifted into the CB, leading to high carrier mobility in the Cr-O co-doped GaN [144].

4.4 ZnO

Owing to its chemical stability and large band-gap (3.2 eV), ZnO is also a candidate photo-catalyst material [145]. Doping and band-gap engineering of wide band-gap ZnO encounter difficulties similar to those encountered for TiO_2 and GaN. Similar to the ADA complex model for GaN [3, 139], the strategy of partially compensated co-doping of Ga, N, and P has been proposed in band-gap engineering of ZnO nanowires [145]. First-principles calculations showed a redshift of the optical absorption spectrum for the co-doped case compared with N mono-doped ZnO, as well as lower defect formation energy, both of which indicate enhanced photo-activity in the partially compensated co-doping scheme [145].

Partially compensated co-doping has also been applied to realizing stable ferromagnetism (FM) in doped ZnO. By performing first-principles calculations, Pan *et al.* found not only enhanced thermodynamic and kinetic incorporation of dopants by using this co-doping strategy, but also stable long-range ferromagnetism owing to the extended states created by the co-doping pairs [144]. They identified Cr-N and V-N as possible co-doping pairs for achieving stable ferromagnetism in ZnO, and scandium-C (Sc-C) co-doped ZnO as a particularly interesting FM semiconductor with net *p*-type conductivity [144].

4.5 ZnS

The ADA complex model has also been applied to ZnS to achieve *p*-type conductivity in this large band-gap semiconductor. For vapor-phase epitaxial ZnS, Kishimoto *et al.* found that (silver(Ag), indium(In), N) triple-doping can largely enhance the free hole concentration and carrier mobility [146]. The photo-luminance spectrum indicated the existence of donor-acceptor pairs, and weak temperature dependence of the hole concentration further hinted that impurity bands were possibly created [146]. Later, Yamamoto *et al.* conducted first-principles calculations and showed that this effect should be attributed to the formation of the N_S-In_{Zn}-N_S complex, which transforms the localized impurity level of N into a delocalized state [147]. Therefore, the enhanced *p*-type conductivity can be explained by the ADA complex model [3, 139].

Also, Muruganandham and Kusumoto found that co-doping C and N into ZnS greatly enhances the visible light absorption compared with undoped ZnS [148]. This finding demonstrates the feasibility of non-metal doped sulfide semiconductors as photo-catalyst materials under visible light irradiation [148]. By performing first-principles calculations, Sun *et al.* showed that the partially compensated N_S-C_i-N_S complex may be formed owing to its low formation energy, and the created impurity states in the middle of the band-gap of ZnS could improve the visible light photo-activity of ZnS [149]. This, too, demonstrates the power of partially compensated co-doping in band-gap engineering of large band-gap semiconductors. Still, co-doping may lower the stability of the host material, which is a key issue in designing photo-catalyst devices.

5 Non-compensated co-doping

Non-compensated co-doping refers to co-doping schemes that do not rely on the energy gain from donor-acceptor pairs to increase the incorporation of dopants. Thus, the mechanisms behind such co-doping schemes were often quite novel. In this section, a few types of materials with different properties will be discussed. First, we will review non-compensated co-doping of TiO_2 for photochemical reactions. In the previous sections, fully and partially compensated co-doping techniques were reviewed. Yet, a third technique was found to effectively increase the device efficiency in the visible light region. It was found that two acceptors, doped at neighboring O sites, can be effective [150, 151]. Second, we will review co-doping of ZnO for improving its *p*-type conductivity and fabrication of diluted magnetic semiconductors (DMSs). Experimental and theoretical calculations showed that co-doping of isovalent Mg_{Zn} or Be_{Zn} with N_O acceptor can effectively reduce the transition level and improve the carrier concentration and conductivity [152, 153]. Manganese (Mn) and N co-doping into ZnO was used for creating room-temperature FM [154, 155]. Third, we will

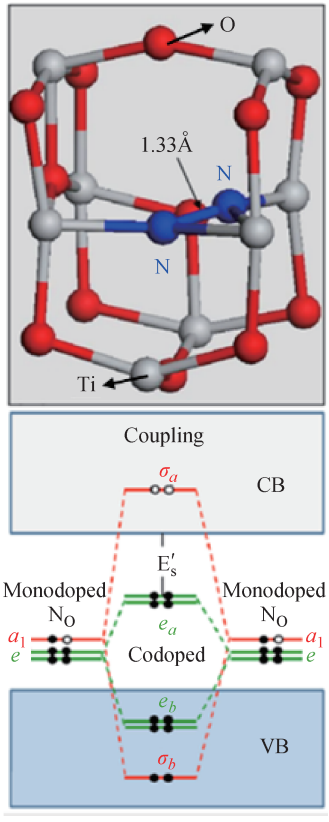

Fig. 3 Structure of (N, N) doped TiO_2 and a schematic diagram of coupling mechanism between two holes from two N_o defects. Reproduced from Ref. [150].

review *p*-doping of ZnS/Se, for improving its *p*-type conductivity, and co-doping of N and tellurium (Te) that was attempted with some success [156].

5.1 Double-hole doping of TiO_2

As was already argued in the previous sections, TiO_2 is one of the most promising materials for the aqueous photocatalytic reaction, yet its application has been hindered by its large band-gap of ∼3.2 eV [157]. Thus,many attempts have been undertaken to dope anion acceptors, such as C, sulfur (S), and N, into TiO_2. Recently, it was found that N mono-doped [158], (C,S) [159] and (N,S/Se) [160] co-doped TiO_2 exhibit redshifts in their absorption spectra. A theoretical explanation of band-gap narrowing by (C,S) co-doping was first suggested by Wang *et al.* [151] and the concept was later generalized by Yin *et al.* [150]. By performing first-principles calculations, they found that two neighboring acceptors at O sites can couple strongly through non-bonding orbitals. The subsequent bonding pushed empty bands into the CBM as anti-bonding states. The coupling between the remaining states of the acceptors created substantial splitting of the filled states and raised some deep band-gap states, substantially reducing the band-gap [150, 151]. Figure 3 schematically shows the co-doped structure and the coupling mechanism. There are ongoing attempts to co-dope cation dopant with the mentioned anions for increasing the efficiencies of photochemical reactions, such as Co-C-S [161] and Fe-N [162], yet, theoretical studies of these complex co-doping schemes are limited. Furthermore, owing to the complex nature of photochemical reactions, the dopant can affect the surface texture and the reaction pathway [150, 157, 161], all of which complicate theoretical studies.

5.2 Isovalent cation and N co-doping of ZnO

Novel methods were also suggested for co-doping wide band-gap semiconductors. Here, we will discuss ZnO as an example. ZnO is a wide band-gap semiconductor with the band gap of ∼3.3 eV. Its hole concentration is low when it is *p*-doped by N_O. Owing to the low solubility of the dopant, compensation of intrinsic *n*-type defects and high transition levels were found [163]. Li *et al.* suggested that *p*–*d* coupling can be removed by Mg_{Zn} or Be_{Zn} substitution sites around the N atom, thus lowering the defect level [152]. Their first-principles calculations showed that the transition level of N_O is 0.31 eV above the VBM, resulting in a low carrier concentration at room temperature. Calculations also showed that the deep level was contributed by the *p*–*d* coupling between the N and Zn atoms. Calculations showed that the N_O-$4Be_{Zn}$ defect complex has the transition energy of 0.12 eV and defect binding energy of 1.9 eV [152]. There was some success with doping N into (Mg, Zn)O, notably by Zhang *et al.* [153]. They created a *p*-type sample with low resistivity ($6.4 \times 10^{-2}\Omega \cdot$ cm), high mobility [11.7 $cm^2/(V \cdot s)$], and high carrier concentration ($8.31 \times 10^{-2} cm^{-3}$), by using ultrasonic spray pyrolysis [153].

Another non-compensated co-doping scheme was created for ZnO in the pursuit of a DMS. Significant body of research focused on doping various transition metals, such as cobalt (Co) and Mn. Because they are chemically isovalent, these metals provide local magnetic moments, but lack charge carriers. It was found that Co and Mn require different polarities of charge carriers to achieve room-temperature FM: *n*-type for Co and *p*-type for Mn [164, 165]. Co-doping of N and Mn into ZnO was also studied theoretically and experimentally [154, 166]. Although the results show FM at room temperature, the exact mechanism for obtaining magnetic ordering remains elusive [155, 167].

5.3 Enhanced *p*-type ZnS by N co-doping with isovalent dopant

The wide band-gaps of ZnS/Se make this material potentially useful as a blue light emitting diode (LED) and a

laser diode [168]. Owing to the intrinsic difficulties associated with p-type doping, co-doping schemes can be appealing. Gaines *et al.* used N-doped $Zn_{1-x}Mg_xS_ySe_{1-y}$ for the cladding layer of a blue-green injection laser [168]. However, this material has a low carrier concentration of 1×10^{17}cm^{-3} [169], and p-ZnSe can only reach the carrier concentration of 1×10^{18}cm^{-3}. To increase the p-type conductivity of ZnS and ZnSe, Jung *et al.* co-doped Te and N into ZnS and ZnSe by using the δ-doping technique and achieved the hole concentration of 10^{20}cm^{-3} [156]. By inserting an N-doped ZnTe layer between undoped ZnS and ZnSe, they successfully increased the hole concentration of ZnSe to 7×10^{18}cm^{-1} and achieved the hole mobility of 10 cm^2/(V·s) at room temperature. However, for ZnS, an Ohmic contact between the doped and undoped layers could not be achieved [156]. Unfortunately, theoretical studies on the mechanism of this co-doping scheme are still largely lacking.

In this section, we review several methods of non-compensated co-doping. It should be noted that these co-doping schemes fall roughly into two categories. The first category involves co-doping multiple anion acceptors such that chemical bonds between these acceptors can be formed, leading to a filled defect state in the band-gap. The band-gap can be modified significantly without introducing carriers into the system. The second category involves co-doping of an isovalent cation dopant with anion acceptors. The doping pair yields different electronic and magnetic properties based on the p–d coupling (or the lack of one) in the cation and its bonding with the anion acceptor.

6 Unintentional co-doping and surface-related co-doping

Although the general discussion and organization of this article follows the logical order of different passivation mechanisms of co-doping, some very important experimental and theoretical works on unintentional co-doping and surface effects on co-doping should be emphasized and will serve as an extension of the general concept of co-doping.

Unintentional co-doping usually happens when unexpected dopant that is present in the growth atmosphere is incorporated into semiconductors, and forms defect complexes with original dopants or intrinsic defects. Background contamination, such as H, C, or O, is often the source of such unexpected dopants [170–172]. In addition, defect complexes of intrinsic defects and dopants can sometimes be regarded as resulting from unintentional co-doping. In this sense, the surface as a special type of defect plays an important role in the incorporation of dopants and surfactant-enhanced doping or co-doping becomes especially interesting.

6.1 Hydrogen co-doping effects

Hydrogen is a common impurity in semiconductors [95, 173–175]. Hydrogen acting as a co-dopant is inevitably incorporated into well-doped semiconductor materials during growth, because many growth techniques include quite a few H atoms, especially OMVPE. One typical example is the famous account of unintentional H impurity co-doping with Mg in GaN, which has been mentioned in Section 2 of this article. Before 1992, it was difficult to achieve good p-type in GaN even after a major breakthrough contributed by Akasaki *et al.* [176]. Nakamura *et al.* found that the electric conductivity of Mg-doped GaN significantly increased after changing the annealing atmosphere from NH_3 to N_2 [177]. Thus, these researchers demonstrated that if Mg is present in the crystal, H atoms (dissociated from NH_3 during growth) form Mg-H complexes, thereby preventing from Mg to act as an acceptor [175, 177]. Thermal annealing of the GaN: Mg sample in an H-free environment above approximately 400 °C allowed H to diffuse out of the crystal, thereby breaking up the Mg-H complexes [175, 177]. A few years later, Neugebauer and van de Walle studied the effects of H and H complexes in GaN [95], by performing first-principles calculations. Their investigation demonstrated that the Mg-H complex has an H-N bond as its main feature, proposing possible mechanisms for H to diffuse out of the p-type regions [95]. Possibilities included diffusion into the substrate material, to the surface, or to extended defects that occur at high concentrations in epitaxial GaN, while the formation of H_2 was excluded because of its high formation energy [95].

In general, H displays a range of complex behaviors when introduced as an impurity in semiconductors. Interstitial H can bind to native defects or to other impurities, often passivating their p- or n-type conductivities [174]. It acts as a donor (H^+) in a p-type material and as an acceptor (H^-) in an n-type material, always counteracting the prevailing conductivity [174]. This depends on whether the transition level, $\varepsilon(+/-)$, intersects the CB or is deep in the energy gap, and H^0, is never thermodynamically stable [174, 178]. Defect-related H effects in semiconductors have been investigated for materials such as Si, Ge, GaAs, and GaP, and this has been extensively reviewed elsewhere [170, 174, 179–181]. Here, we describe only some recent progresses. For Si, new defect configurations of H/Si complexes [182] and H/N/O defect [183] complexes in Si have been theoretically discovered, yielding new insights into H-related dopant effects in Si. For compound semiconductors, the N-H and other H-induced defect complexes, interacting with intrinsic defects, were reported for GaNP, GaNAs, GaSb,

and InN [184–189]. This indicates that H activates new defects [187] and tunes band-gaps [188] in such materials. Also in oxides, H-related defects were revealed to passivate C or N contamination by forming C-H or N-H complexes in Al_2O_3 [190]. A theoretical study demonstrated that H exhibits amphoteric behavior by forming complexes with intrinsic and extrinsic defects in ZnO [191]. It can also passivate N-related acceptors in ZnO by forming neutral defect complexes [192, 193]. In addition, H helps suppress sodium (Na) interstitials to enhance Na-doped *p*-type ZnO [194]. For TiO_2 in the rutile phase it was reported that H behaves as a deep donor in rutile and always forms an OH^+ complex, independent of the Fermi energy [195]. It can also form a stable H_O-V_O complex, still behaving as a deep donor [195]. Such behavior distinguishes H in TiO_2 from H in other semiconductors [195]. Besides, Pan *et al.* proposed that H acting as a co-dopant with N into anatase and brookite TiO_2 improves their photocatalytic performance [196], owing to the enhancement of absorption and reduction of recombination centers [196].

Effects of unintentionally doped H in DMSs were also investigated within the framework of DFT. The results suggest that interstitial H enhances the magnetic properties of ZnO:Co by the formation of a bridge bond for a spin–spin interaction among Co ions [197]. Besides, the role of H_O is also important, as stable Co-H_O-Co complexes would be formed. The formation of such complexes opens a channel for strong FM coupling by short-range exchange interaction with Co ions [198]. Also in (Mn, N)-co-doped ZnO, it may favor an -Mn-H-N- complex with the existence of H [199]. The strong hybridization between the H-impurity band and the 3*d* minority spin states of Mn at the Fermi level in the gap results in the FM coupling between the spins of Mn and N [199]. Hydrogen-dopant effects were also observed in some experiments [200–202] for DMS material systems. Except for semiconductors, the problem of H embrittlement for high-strength steels and Al alloys is also a crucial issue in modern materials physics [203]. By conducting first-principles calculations, it was revealed that vacancies in metals, such as Al, palladium (Pd), bcc-Fe, fcc-Fe, could trap from 5 to 12 H atoms [203–206], forming H-vacancy complexes. It was found that for H-rich conditions there is a dramatic increase in the vacancy concentration in the fcc-Fe [203]. These findings indicate the importance of vacancy-interstitial complexes in such systems.

6.2 Carbon co-doping effects

In addition, C is one of unintentional impurities that is especially found in the compounds that are grown by performing OMVPE. Decades ago, Theis *et al.* observed the substitutional C impurity in GaAs [207]. Carbon in OMVPE has been studied as both an unintentional and intentional dopant for a long time [171]. Carbon is an amphoteric dopant, which has been systematically investigated in AlN, GaN, InN, AlSb, and GaInNAs, to name a few [96, 208–214]. In GaN, for example, C-related defects are the likely origin of the yellow luminescence (YL) [212, 214], which is frequently observed.

Recently, the effects of unintentionally doped C in ZnO by OMVPE growth have attracted significant attention [215–219], in studies that attempted to suppress the incorporation of C for achieving high-performance *p*-type N-doped ZnO. Experimentally, it was reported that C *sp2* clusters, which are graphite-like along grain boundaries [220, 221], were found in undoped [217, 222] and N-doped ZnO [216, 221, 222]. This indicated that defect complexes of CH_x, NH_x, and NC_x were likely to be present [193], with C concentration significantly increasing in N-doped samples [193, 223, 224]. This suggested that unintentionally doped C impurities prefer to form defect complexes with N [193, 223, 224]. Theoretically, $(N_O–H)^0$ and $(NC)_O^{1+}$ defect complexes were predicted to have low formation energies [193]. The formation energy of the $(NC)_O^{1+}$ defect complex is lower than that of a single C interstitial [223]. This implies that C is one of the possible passivation factors of the N acceptor [225]. This effect was also observed in (Mn, N)-co-doped ZnO, with weakened spin polarization induced by unintentionally incorporated carbon [226]. On the other hand, Tan *et al.* observed *p*-type conduction in unintentionally C-doped ZnO by OMVPE, and proposed that the C-O defect: $(C_{Zn}+2O_i)$ complex would preferentially appear in O-poor annealing ambient, acting as a shallow donor with the transition level of ∼57 meV [227].

6.3 Other impurities

Much research has concentrated on the effects of unintentional oxygen doping into semiconductors [172, 228–232], especially GaN [229, 231, 232] and AlGaN [172, 230]. Similar co-doping effects were demonstrated. For example, it was reported recently that unintentionally doped O in europium-doped (Eu-doped) GaN played an integral role in the location, stability, and local defect structure around the Eu ions [232]. The formation of these Eu-O complexes appears to be more beneficial to the crystal quality and stability than either defect is on its own [232]. Actually, during the growth of nitrides and oxides, unintentional As and B impurities were also observed [233–235].

6.4 Intrinsic defect complexes

Intrinsic defect complexes or complexes of intrinsic defects and dopants are often formed unexpectedly in ex-

periments. First-principles calculations may help to understand the physical mechanisms underlying the formation of such complexes during growth. For instance, in ZnO, intrinsic defect complexes were present deep in the band-gap and were responsible for the observed luminescence peak in ZnO [236]. It was proposed that the often-observed green luminescence may result from the (V_O + V_{Zn}) defect complex [236]. Further, it was proposed that the red/orange luminescence found in Zn-rich samples can arise from ZnO defects [236]. It was also proposed that YL may be caused by the (V_O + V_{Zn}) defect complex [236]. Theoretical models of N_O, V_O, and Zn_i were also proposed for ZnO, such as $2N_O$-Zn_i, $2N_O$-V_O, and $4N_O$-V_O-Zn_i [237], which produce the appropriate electronic structures ready for enhanced visible absorption and H_2 generation from water [237]. Yet, charge-compensated intrinsic defect complexes were reported in Cu_2ZnSnS_4 [238], which were calculated to have low formation energies and be able to passivate the deep donor levels. Such models may give rise to electrically benign characteristics of thin-film Cu_2ZnSnS_4 solar cells [238].

In light of the aforementioned facts, we can conclude that: (i) background impurities are important factors determining the characteristic of semiconductors; they should be carefully controlled and considered, possibly exhibiting passivation effects; (ii) the investigations of intrinsic defects and defect complexes and their interactions with extrinsic dopants are crucial for achieving ideal material performance.

6.5 Surfactant-enhanced doping

In addition to the co-doping mechanisms in bulk crystals, surfactant-enhanced doping is a novel strategy, and can be considered as an extension of the general concept of co-doping. The only difference is that one of the co-doping elements is present on the surface.

Surfactants are defined as elements that always float atop the thin-film surface. They have been widely used in epitaxial growth for controlling growth thermodynamics and kinetics [239–247], and hence for improving crystal qualities and device performance. Recently, surfactants were found to enhance the doping of semiconductors [248-252].

Experimentally, it was found that Sb can enhance the incorporation of Zn into InGaP and GaP [248, 253]. Howard *et al.* used Sb and bismuth (Bi) as surfactants to enhance the incorporation of Zn into InGaP during the OMVPE growth [253]. Hydrogen also plays a role in the doping process [253]. When Sb is incorporated into the growth process, both H and Zn concentrations increase [253]. The physical mechanism of surfactant-enhanced doping remained unclear at that time.

In 2008, Zhu *et al.* discovered the dual surfactant effect of Sb and H for enhancing the *p*-type doping in GaP [249]. They found that the formation energy of Zn_{Ga} can be significantly lowered only when both Sb and H are present, as shown in Fig. 4. Antimony acts as an electron reservoir and H provides the extra electron to fill the reservoir and later transfer the electron to the Zn_{Ga} acceptor, thus lowering the dopant formation energy. Further, Zhu *et al.* extended their model to other metallic *p*-type dopants in GaP, such as Mg, beryllium (Be), and cadmium (Cd) [252]. They found that Mg is the most metallic and may help in the electron redistribution and in reducing the electron reservoir effect.

Later, surfactant-enhanced doping was demonstrated in many semiconductor systems. Sato *et al.* reported that Sb as a surfactant can enhance the Zn doping in InGaAs by OMVPE, yielding a carrier concentration as high as 6.5×10^{19} cm^{-3} [254]. They concluded that Sb enhanced surface diffusion of Zn [254, 255] and increased the Zn atom activation rate at a low growth temperature [254]. For InAs, Wagener *et al.* observed that the surfactant action of a small mole fraction of Sb increased the maximal *p*-type doping density twofold; this study was performed by using OMVPE and dimethyl cadmium as a *p*-type dopant source [256].

Zhang *et al.* theoretically modeled the dual surfactant effects from the perspective of electronic structures, for Sb and H. They pointed out that when P is replaced by the Sb surfactant, the high *p*-orbital energy of Sb provides a high level that could transfer electrons to the dopant level and lower the dopant formation energy. However, because Sb is isovalent to P, H is needed here to provide electrons to occupy the surfactant level that makes the electron transfer to the lower dopant level possible. They also pointed out that H is only needed when the higher level introduced by the surfactant is empty [251, 255]. In addition, they explained the effect of Te on the *p*-type doping of ZnSe, and predicted that ZnO *p*-type doping can be enhanced by silver (Ag) through

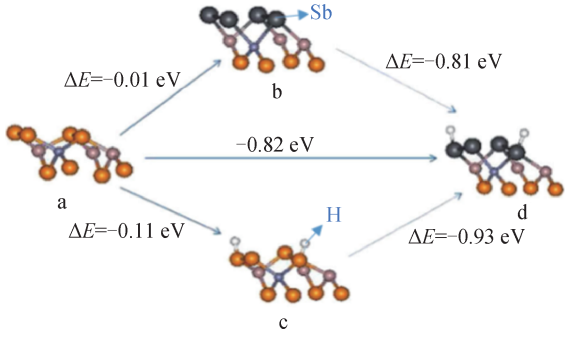

Fig. 4 Schematic illustration of Zn doping in different surfactant configurations. Part (d) shows the dual surfactant case, which has the lowest formation energy of Zn_{Ga}. Reproduced from Ref. [249].

dual surfactants S and Te, together with H [251]. This hypothesis remains to be validated.

Surfactant-enhanced doping may also have some kinetic effects. Kahwaji *et al.* observed that lead (Pb) as a surfactant significantly affected the structural and magnetic properties of the sub-monolayer of Mn in Mn δ-doped layers in Si(001) growth, and also showed, from the theoretical point of view, that Pb changed the pathway for Mn to access the Si substitutional sites and enabled substitutional incorporation by lowering the formation energy of Si vacancies [257].

Surfactants also induced different strain sites around themselves in the growth front of epitaxial grown thin films. It is expected that an external strain that deforms the host lattice may reduce the dopant-induced strain, thus reducing the dopant formation energy [255, 258]. Thus, a tensile strain may enhance the interstitial doping and a compressive strain may reduce the interstitial doping [255, 259]. In addition, the size compensation effect can be a critical issue for choosing co-doping pairs. Ideal co-doping can be achieved only when both the size and electronic compensation are tuned and optimized. For example, group VII elements were proposed as effective co-dopants to help f electron metal elements doped in topological insulators owing to both the size and electronic compensation effects [260]. Another size-tuning example of surfactants is the study of Sb-enhanced In incorporation in InGaN. Antimony as a surfactant was found to largely enhance the incorporation of Ininto InGaN [261], which is also owing to the surfactant-induced strain effect [262]. Merrell *et al.* found that an abrupt increase in the concentration of In was achieved by adding a small amount of Sb on InGaN surfaces during OMVPE growth [261]. Recently, Zhang *et al.* studied this phenomenon theoretically by conducting first-principles calculations, and found that under different surface reconstructions, the surface stress analysis indicates that Sb adatoms on H3 sites lead to tensile sites in the GaN bilayer, which can enhance the incorporation of In by lowering the formation energy of In_{Ga} [262].

7 Summary and outlook

We reviewed co-doping methods for different compensating mechanisms, as well as contamination and surfactant effects. In general, co-doping may enhance the stability of defects, increase the solubility of impurities, and thus improve the conductivities of corresponding materials. However, many questions related to co-doping remain open. Co-doping may destabilize some crystals, form unwanted defects or defect complexes, introduce detrimental mid-gap bands, deactivate certain wanted defects or dopants. Therefore, there is often a compromise between the enhanced electronic properties and the drawbacks of the above-mentioned co-doping methods. One important application of co-doping is to improve the magnetic properties, which is especially important in DMS and topological insulators. Co-doping may be the method of choice for incorporating a large amount of magnetic dopants for forming a long-range magnetic order. Due to the limited length of the paper, we were not able to provide a detailed review of this problem. Yet, all these challenges and potential improvements in device physics based on co-doping methods call for more systematic and creative research efforts.

Acknowledgements This work was supported by the start-up funding, direct grant with the Project code of 4053134 at CUHK and ECS grant from HKRGC (Grant No. 24300814).

References

1. C. Freysoldt, B. Grabowski, T. Hickel, J. Neugebauer, G. Kresse, A. Janotti, and C. G. Van de Walle, First-principles calculations for point defects in solids, *Rev. Mod. Phys.* 86(1), 253 (2014)
2. S. Wei, Overcoming the doping bottleneck in semiconductors, *Comput. Mater. Sci.* 30(3–4), 337 (2004)
3. H. Katayama-Yoshida, T. Nishimatsu, T. Yamamoto, and N. Orita, Codoping method for the fabrication of low-resistivity wide band-gap semiconductors in p-type GaN, p-type AlN and n-type diamond: Prediction versus experiment, *J. Phys.: Condens. Matter* 13(40), 8901 (2001)
4. U. Kaufmann, P. Schlotter, H. Obloh, K. Köhler, and M. Maier, Hole conductivity and compensation in epitaxial GaN:Mg layers, *Phys. Rev. B* 62(16), 10867 (2000)
5. R. Korotkov, J. Gregie, and B. Wessels, Electrical properties of p-type GaN:Mg codoped with oxygen, *Appl. Phys. Lett.* 78(2), 222 (2001)
6. G. Kipshidze, V. Kuryatkov, B. Borisov, Y. Kudryavtsev, R. Asomoza, S. Nikishin, and H. Temkin, Mg and O codoping in p-type GaN and $Al_xGa_{1-x}N$ ($0< x <0.08$), *Appl. Phys. Lett.* 80(16), 2910 (2002)
7. B. Gudden, On electrical conduction in semiconductors, *Sitzungsberichte der Physikalisch-medizinischen Sozietat zu Erlangen*, 62, 289 (1930)
8. P. R. Morris, A history of the world semiconductor industry, IET Digital Library (1990)

9. A. H. Wilson, The theory of electronic semi-conductors, *Proceedings of the Royal Society A*, 133(822), 458 (1931)
10. L. Grondahl and P. H. Geiger, A new electronic rectifier, *Transactions of the American Institute of Electrical Engineers*, 46, 357 (1927)
11. C. E. Fritts, On a new form of selenium cell, and some electrical discoveries made by its use, *Am. J. Sci.* s3-26 (156), 465 (1883)
12. J. Preston, The selenium rectifier photocell: Manufacture, properties, and use in photometry, *Journal of the Institution of Electrical Engineers* 79(478), 424 (1936)
13. B. Davydov, The rectifying action of semiconductors, *Technical Physics of the USSR* 5, 87 (1938)
14. J. R. Woodyard, Nonlinear circuit device utilizing germanium, US2530110[P] (1950)
15. W. Shockley, The theory of *p–n* junctions in semiconductors and *p–n* junction transistors, *Bell Syst. Tech. J.* 28(3), 435 (1949)
16. H. Choi, The boundaries of industrial research: Making transistors at RCA, 1948–1960, *Technol. Cult.* 48(4), 758 (2007)
17. G. Teal, M. Sparks, and E. Buehler, Growth of germanium single crystals containing *p–n* junctions, *Phys. Rev.* 81(4), 637 (1951)
18. M. Sparks, Method of making *p–n* junctions, US2631356A[P] (1953)
19. C. S. Fuller, Diffusion of donor and acceptor elements into germanium, *Phys. Rev.* 86(1), 136 (1952)
20. C. Fuller and J. Ditzenberger, Diffusion of lithium into germanium and silicon, *Phys. Rev.* 91(1), 193 (1953)
21. H. Reiss, Chemical effects due to the ionization of impurities in semiconductors, *J. Chem. Phys.* 21(7), 1209 (1953)
22. H. Reiss, C. Fuller, and A. Pietruszkiewicz, Solubility of lithium in doped and undoped silicon, evidence for compound formation, *J. Chem. Phys.* 25(4), 650 (1956)
23. H. Reiss, C. Fuller, and F. Morin, Chemical interactions among defects in germanium and silicon, *Bell Syst. Tech. J.* 35(3), 535 (1956)
24. F. Kröger and H. Vink, Relations between the concentrations of imperfections in crystalline solids, *Solid State Phys.* 3, 307 (1956)
25. F. Kröger and H. Vink, Relations between the concentrations of imperfections in solids, *J. Phys. Chem. Solids* 5(3), 208 (1958)
26. J. Maita, Ion pairing in silicon, *J. Phys. Chem. Solids* 4(1–2), 68 (1958)
27. H. Reiss and C. Fuller, The effect of ion pair and ion triplet formation on the solubility of lithium in germanium — effect of gallium and zinc, *J. Phys. Chem. Solids* 4(1–2), 58 (1958)
28. R. Korotkov, J. Gregie, and B. Wessels, Codoping of wide gap epitaxial III-Nitride semiconductors, *Opto-Electron. Rev.* 4, 243 (2002)
29. W. Shockley and J. Moll, Solubility of flaws in heavily-doped semiconductors, *Phys. Rev.* 119(5), 1480 (1960)
30. E. Mahlab, V. Volterra, W. Low, and A. Yariv, Orthorhombic electron spin resonance spectrum of U3 in CaF_2, *Phys. Rev.* 131(3), 920 (1963)
31. P. Weller and J. Scardefield, Doping of alkaline earth halide single crystals, *J. Electrochem. Soc.* 111(8), 1009 (1964)
32. M. Taylor, An experimental study of the efficiency of optical energy transfer between Cr_3 and Nd_3 ions in yttrium aluminium garnet, *Proc. Phys. Soc.* 90(2), 487 (1967)
33. G. Blasse and A. Bril, Energy transfer from trivalent rare earth ions to Cr_3, *Phys. Lett. A* 25(1), 29 (1967)
34. J. Axe and P. Weller, Fluorescence and energy transfer in Y_2O_3:Eu_3, *J. Chem. Phys.* 40(10), 3066 (1964)
35. M. Brown, J. Whiting, and W. Shand, Ion-ion interactions in rare-earth-doped LaF_3, *J. Chem. Phys.* 43(1), 1 (1965)
36. H. Rast, H. Caspers, and S. Miller, Fluorescence and energy transfer between Nd_3 and Yb_3 in LaF_3, *J. Chem. Phys.* 47(10), 3874 (1967)
37. C. Asawa, Long-delayed fluorescence of Nd_3 in pure $LaCl_3$ and in $LaCl_3$ containing Ce_3, *Phys. Rev.* 155(2), 188 (1967)
38. E. J. Sharp, M. J. Weber, and G. Cleek, Energy transfer and fluorescence quenching in Eu-and Nd-doped silicate glasses, *J. Appl. Phys.* 41(1), 364 (1970)
39. N. Melamed, C. Hirayama, and P. French, Laser action in uranyl-sensitized Nd-doped glass, *Appl. Phys. Lett.* 6(3), 43 (1965)
40. E. Snitzer and R. Woodcock, 9C8 - Saturable absorption of color centers in Nd^{3+} and Nd^{3+}-Yb^{3+} laser glass, *IEEE J. Quantum Electron.* 2(9), 627 (1966)
41. H. Gandy, R. Ginther, and J. Weller, Internal *Q* switching of Ho_3-Stimulated emission in iron-containing glasses, *Appl. Phys. Lett.* 9(8), 277 (1966)
42. L. Erickson and A. Szabo, Behavior of saturable-absorber giant-pulse lasers in the limit of large absorber cross section, *J. Appl. Phys.* 38(6), 2540 (1967)
43. P. F. Weller, Optical spectra of ytterbium in CdF_2, *J. Electrochem. Soc.* 114(6), 609 (1967)
44. J. L. Wolf and P. P. Yaney, The enhancement of the 6P(7/2) fluorescence of Gd(3) in SrF_2 containing Ce(3+) as a codopant, Rept. No. UDRI-TR-69-34 (1970)
45. A. Lyall, H. Seiger, and R. Shair, Lithium-nickel Halide Secondary Battery Investigation (1966)
46. M. Balkanski and W. Nazarewicz, Infrared study of localized vibrations in silicon due to boron and lithium, *J. Phys. Chem. Solids* 27(4), 671 (1966)
47. B. Faughnan and Z. Kiss, Photoinduced reversible charge-transfer processes in transition-metal-doped single-crystal $SrTiO_3$ and TiO_2, *Phys. Rev. Lett.* 21(18), 1331 (1968)

48. B. W. Faughnan and Z. J. Kiss, Optical and EPR studies of photochromic $SrTiO_3$ doped with Fe/Mo and Ni/Mo, *IEEE J. Quantum Electron.* 5, 17 (1969)

49. D. Thomas, M. Gershenzon, and F. Trumbore, Pair spectra and "edge" emission in gallium phosphide, *Phys. Rev.* 133(1A), A269 (1964)

50. L. Foster and J. Scardefield, Oxygen doping of solution-grown gaP, *J. Electrochem. Soc.* 116(4), 494 (1969)

51. H. Komiya, Optical spectra of Tm_3 ions in ZnSe:Tm, Li and ZnSe:Tm, Cu crystals, *J. Phys. Soc. Jpn.* 27(4), 893 (1969)

52. S. Ibuki, H. Komiya, M. Nakada, H. Masui, and H. Kimura, Investigation of rare earth ions in ZnSe, *J. Lumin.* 1–2, 797 (1970)

53. H. Kukimoto, S. Shionoya, T. Koda, and R. Hioki, Infrared absorption due to donor states in ZnS crystals, *J. Phys. Chem. Solids* 29(6), 935 (1968)

54. J. Apperson, G. Garlick, W. Lamb, and B. Lunn, Luminescence properties of rare earth activated cadmium sulphide in the range 4000 to 15000 cm^{-1}, *Physica Status Solidi (b)* 34, 537 (1969)

55. L. Miller, Properties of Elemental and Compound Semiconductors, New York: Interscience, 1960, p. 303

56. C. Fuller, F. Doleiden, and K. Wolfstirn, Reactions of group III acceptors with oxygen in silicon crystals, *J. Phys. Chem. Solids* 13(3-4), 187 (1960)

57. R. Chrenko, R. McDonald, and E. Pell, Vibrational spectra of lithium-oxygen and lithium-boron complexes in silicon, *Phys. Rev.* 138(6A), A1775 (1965)

58. A. Cosand and W. Spitzer, Localized vibrational modes of Li and P impurities in germanium, *Appl. Phys. Lett.* 11(9), 279 (1967)

59. J. Lawrence, The cooperative diffusion effect, *J. Appl. Phys.* 37(11), 4106 (1966)

60. W. Wilcox, T. LaChapelle, and D. Forbes, Gold in silicon: Effect on resistivity and diffusion in heavily-doped layers, *J. Electrochem. Soc.* 111(12), 1377 (1964)

61. M. Joshi and S. Dash, Distribution and precipitation of gold in phosphorus-diffused silicon, *J. Appl. Phys.* 37(6), 2453 (1966)

62. W. Bullis, Properties of gold in silicon, *Solid-State Electron.* 9(2), 143 (1966)

63. R. D. Baxter, R. Bate, and F. Reid, Ion-pairing between lithium and the residual acceptors in GaSb, *J. Phys. Chem. Solids* 26(1), 41 (1965)

64. W. Hayes, Localized vibrations of lithium complexes in gallium arsenide, *Phys. Rev.* 138(4A), A1227 (1965)

65. L. Riseberg and W. Holton, Nd ion site distribution and spectral line broadening in YA1G:Lu, Nd laser materials, *J. Appl. Phys.* 43(4), 1876 (1972)

66. R. Hotz, Thermal transient effects in repetitively pulsed flashlamp-pumped YAG:Nd and YAG:Nd, Lu laser material, *Appl. Opt.* 12(8), 1834 (1973)

67. J. Kvapil, J. Kvapil, and B. Perner, O^- centre formation in yag crystals doped with rare earth ions, *Kristall und Technik* 10(2), 161 (1975)

68. J. Falk, L. Huff, and J. Taynai, Solar-pumped, mode-locked, frequency-doubled Nd:YAG laser, *IEEE J. Quantum Electron.* 11(9), 836 (1975)

69. Y. K. Voronko and A. Sobol, Classification and analysis of the impurity ion clusters in $Y_3AI_5O_{12}$, *Physica Status Solidi (a)* 27, 257 (1975)

70. R. A. Hewes and J. F. Sarver, Infrared excitation processes for the visible luminescence of Er_3, Ho_3, and Tm_3 in Yb_3-sensitized rare-earth trifluorides, *Phys. Rev.* 182(2), 427 (1969)

71. G. Ban and H. Hersh, Degradation of some IR upconverting phosphors by ionizing radiation, *J. Electron. Mater.* 1(2), 320 (1972)

72. S. Zenbutu, R. Nakata, M. Sumita, and E. Higuchi, EPR study of characteristics of Fe_3 ions with cubic symmetry in CaF_2 crystals, *Jpn. J. Appl. Phys.* 10(11), 1497 (1971)

73. P. P. Yaney, D. M. Schaeffer, and J. L. Wolf, Fluorescence and absorption studies of $Sr_{0.999-x}Gd_{0.001}Ce_xF_{2.001+x}$, *Phys. Rev. B* 11(7), 2460 (1975)

74. G. Miner, T. Graham, and G. Johnston, Effect of a Ce_3 codopant on the Gd_3 EPR spectrum of SrF_2 at room temperature, *J. Chem. Phys.* 57(3), 1263 (1972)

75. P. Dean, Isoelectronic trap Li-Li-O in GaP, *Phys. Rev. B* 4(8), 2596 (1971)

76. J. Wiley, Donor-acceptor pairing in the system GaP(Zn, O), *J. Phys. Chem. Solids* 32(9), 2053 (1971)

77. V. Swaminathan and L. Greene, Pair spectra, edge emission, and the shallow acceptors in melt-grown ZnSe, *Phys. Rev. B* 14(12), 5351 (1976)

78. H. Woodbury, Anomalous mobility behavior in CdS and CdTe: Electrical evidence for impurity pairs, *Phys. Rev. B*9(12), 5188 (1974)

79. K. Arai, H. Namikawa, K. Kumata, T. Honda, Y. Ishii, and T. Handa, Aluminum or phosphorus co-doping effects on the fluorescence and structural properties of neodymium-doped silica glass, *J. Appl. Phys.* 59(10), 3430 (1986)

80. Y. Ishii, K. Arai, H. Namikawa, M. Tanaka, A. Negishi, and T. Handa, Preparation of cerium-activated silica glasses: Phosphorus and aluminum codoping effects on absorption and fluorescence properties, *J. Am. Ceram. Soc.* 70(2), 72 (1987)

81. S. G. Kosinski, D. M. Krol, T. Duncan, D. Douglas, J. MacChesney, and J. Simpson, Raman and NMR spectroscopy of SiO_2 glasses co-doped with Al_2O_3 and P_2O_5, *J. Non-Cryst. Solids* 105(1–2), 45 (1988)

82. C. A. Millar, B. Ainslie, I. Miller, and S. Craig, Concentration and co-doping dependence of the $4F_{3/2}$ to $4/I_{11/2}$ lasing behavior of Nd^{3+} silica fibers, *Zhurnal Mikrobiologii Epidemiologii I Immunobiologii*, 72(2), 113-5 (1995)

83. V. Rakovics, R. Fornari, C. Paorici, L. Zanotti, and C. Mucchino, Indium-silicon co-doping effects in LEC-Grown gallium arsenide crystals, *Acta Phys. Hung.* 61, 255 (1987)

84. H. Miyairi, T. Inada, M. Eguchi, and T. Fukuda, Growth and properties of InP single crystals grown by the magnetic field applied LEC method, *J. Cryst. Growth* 79(1–3), 291 (1986)

85. B. Lambert, Y. Toudic, G. Grandpierre, M. Gauneau, and B. Deveaud, Semi-insulating InP co-doped with Ti and Hg, *Semicond. Sci. Technol.* 2(2), 78 (1987)

86. Y. Toudic, R. Coquille, M. Gauneau, G. Grandpierre, L. Le Marechal, and B. Lambert, Growth of double doped semi-insulating indium phosphide single crystals, *J. Cryst. Growth* 83(2), 184 (1987)

87. A. Katsui, Thermal stability of (Ti Zn)-co-doped semi-insulating InP single crystals, *J. Cryst. Growth* 89(4), 612 (1988)

88. R. Fornari, J. Kumar, M. Curti, and G. Zuccalli, Growth and properties of bulk indium phosphide doubly doped with cadmium and sulphur, *J. Cryst. Growth* 96(4), 795 (1989)

89. A. G. Dentai and C. H. JoynerJr, Semiconductor devices employing Ti-doped Group III-V epitaxial layer, US4774554[P] (1988)

90. J. Zhu, N. Johnson, and C. Herring, Negative-charge state of hydrogen in silicon, *Phys. Rev. B* 41(17), 12354 (1990)

91. E. Ö. Sveinbjörnsson and O. Engström, Reaction kinetics of hydrogen-gold complexes in silicon, *Phys. Rev. B*52(7), 4884 (1995)

92. A. A. Istratov, C. Flink, H. Hieslmair, E. R. Weber, and T. Heiser, Intrinsic diffusion coefficient of interstitial copper in silicon, *Phys. Rev. Lett.* 81(6), 1243 (1998)

93. S. McHugo, R. McDonald, A. Smith, D. Hurley, and E. Weber, Iron solubility in highly boron-doped silicon, *Appl. Phys. Lett.* 73(10), 1424 (1998)

94. A. Istratov, H. Hieslmair, and E. Weber, Iron and its complexes in silicon, *Appl. Phys. A* 69(1), 13 (1999)

95. J. Neugebauer and C. G. Van de Walle, Hydrogen in GaN: Novel aspects of a common impurity, *Phys. Rev. Lett.* 75(24), 4452 (1995)

96. P. Bogusl?awski, E. L. Briggs, and J. Bernholc, Amphoteric properties of substitutional carbon impurity in GaN and AlN, *Appl. Phys. Lett.* 69(2), 233 (1996)

97. D. Chadi, Doping in ZnSe, ZnTe, MgSe, and MgTe wide-band-gap semiconductors, *Phys. Rev. Lett.* 72(4), 534 (1994)

98. S. Zhang, S. Wei, and A. Zunger, Overcoming doping bottlenecks in semiconductors and wide-gap materials, *Physica B* 273–274, 976 (1999)

99. W. Walukiewicz, Intrinsic limitations to the doping of wide-gap semiconductors, *Physica B* 302–303, 123 (2001)

100. S. Zhang, The microscopic origin of the doping limits in semiconductors and wide-gap materials and recent developments in overcoming these limits: A review, *J. Phys.: Condens. Matter* 14(34), R881 (2002)

101. Y. Gai, J. Li, S. Li, J. Xia, and S. Wei, Design of narrow-gap TiO_2: A passivated codoping approach for enhanced photoelectrochemical activity, *Phys. Rev. Lett.* 102(3), 036402 (2009)

102. J. Zhang, C. Pan, P. Fang, J. Wei, and R. Xiong, Mo C codoped TiO_2 using thermal oxidation for enhancing photocatalytic activity, *ACS Appl. Mater. Interfaces* 2(4), 1173 (2010)

103. R. Long and N. J. English, Tailoring the electronic structure of TiO_2 by cation codoping from hybrid density functional theory calculations, *Phys. Rev. B* 83(15), 155209 (2011)

104. O. Khaselev and J. A. Turner, A monolithic photovoltaic-photoelectrochemical device for hydrogen production via water splitting, *Science* 280(5362), 425 (1998)

105. R. Long and N. J. English, Band gap engineering of (N, Ta)-codoped TiO_2: A first-principles calculation, *Chem. Phys. Lett.* 478(4–6), 175 (2009)

106. R. Long and N. J. English, Synergistic effects on band gap-narrowing in titania by codoping from first-principles calculations, *Chem. Mater.* 22(5), 1616 (2010)

107. T. M. Breault and B. M. Bartlett, Lowering the band gap of anatase-structured TiO_2 by coalloying with Nb and N: Electronic structure and photocatalytic degradation of methylene blue dye, *J. Phys. Chem. C* 116(10), 5986 (2012)

108. P. Dong, B. Liu, Y. Wang, H. Pei, and S. Yin, Enhanced photocatalytic activity of (Mo, C)-codoped anatase TiO_2 nanoparticles for degradation of methyl orange under simulated solar irradiation, *J. Mater. Res.* 25(12), 2392 (2010)

109. E. M. Neville, M. J. Mattle, D. Loughrey, B. Rajesh, M. Rahman, J. D. MacElroy, J. A. Sullivan, and K. R. Thampi, Carbon-doped TiO_2 and carbon, tungsten-codoped Tio_2 through sol–gel processes in the presence of melamine borate: Reflections through photocatalysis, *J. Phys. Chem. C* 116(31), 16511 (2012)

110. Q. Xiao and L. Gao, One-step hydrothermal synthesis of C, W-codoped mesoporous TiO_2 with enhanced visible light photocatalytic activity, *J. Alloys Compd.* 551, 286 (2013)

111. J. Xu, C. Chen, X. Xiao, L. Liao, L. Miao, W. Wu, F. Mei, A. L. Stepanov, G. Cai, Y. Liu, Z. Dai, F. Ren, C. Jiang, and J. Liu, Synergistic effect of V/N codoping by ion implantation on the electronic and optical properties of TiO_2, *J. Appl. Phys.* 115(14), 143106 (2014)

112. X. Ma, Y. Wu, Y. Lu, J. Xu, Y. Wang, and Y. Zhu, Effect of compensated codoping on the photoelectrochemical properties of anatase TiO_2 photocatalyst, *J. Phys. Chem. C* 115(34), 16963 (2011)

113. R. Long and N. J. English, Band gap engineering of double-cation-impurity-doped anatase-titania for visible-light photocatalysts: A hybrid density functional theory approach, *Phys. Chem. Chem. Phys.* 13(30), 13698 (2011)

114. R. Long and N. J. English, Electronic structure of cation-codoped TiO_2 for visible-light photocatalyst applications from hybrid density functional theory calculations, *Appl. Phys. Lett.* 98(14), 142103 (2011)

115. H. Irie, Y. Watanabe, and K. Hashimoto, Nitrogen-concentration dependence on photocatalytic activity of $TiO_{2-x}N_x$ powders, *J. Phys. Chem. B* 107(23), 5483 (2003)

116. J. Neugebauer and C. G. Van de Walle, Role of hydrogen in doping of GaN, *Appl. Phys. Lett.* 68(13), 1829 (1996)

117. S. Nakamura, T. Mukai, M. Senoh, and N. Iwasa, Thermal annealing effects on p-type Mg-doped GaN films, *Jpn. J. Appl. Phys.* 31, L139 (1992)

118. W. Zhu, X. Qiu, V. Iancu, X. Chen, H. Pan, W. Wang, N. M. Dimitrijevic, T. Rajh, Meyer, M. P. Paranthaman, G. M. Stocks, H. H. Weitering, B. Gu, G. Eres, and Z. Zhang, Band gap narrowing of titanium oxide semiconductors by noncompensated anion-cation codoping for enhanced visible-light photoactivity, *Phys. Rev. Lett.* 103(22), 226401 (2009)

119. F. Wu, H. Lan, Z. Zhang, and P. Cui, Quantum efficiency of intermediate-band solar cells based on non-compensated np codoped TiO_2, *J. Chem. Phys.* 137(10), 104702 (2012)

120. X. Li, G. Wu, G. Zhong, W. Li, G. Lu, C. Yang, X. Xiao, and Z. Zhang, Single element non-compensate np co-doped $CuAlSe_2$ as candidate materials for intermediate-band solar cells (2015)

121. M. Han, X. Zhang, Y. Zhang, and Z. Zeng, The group VA element non-compensated n–p codoping in $CuGaS_2$ for intermediate band materials, *Sol. Energy Mater. Sol. Cells* 144, 664 (2016)

122. A. Fujishima and K. Honda, Electrochemical photolysis of water at a semiconductor electrode, *Nature* 238(5358), 37 (1972)

123. M. Grätzel, Photoelectrochemical cells, *Nature* 414 (6861), 338 (2001)

124. R. Asahi, T. Morikawa, T. Ohwaki, K. Aoki, and Y. Taga, Visible-light photocatalysis in nitrogen-doped titanium oxides, *Science* 293(5528), 269 (2001)

125. A. Luque and A. Martí, Increasing the efficiency of ideal solar cells by photon induced transitions at intermediate levels, *Phys. Rev. Lett.* 78(26), 5014 (1997)

126. M. E. Kurtoglu, T. Longenbach, K. Sohlberg, and Y. Gogotsi, Strong coupling of Cr and N in Cr–N-doped TiO_2 and its effect on photocatalytic activity, *J. Phys. Chem. C* 115(35), 17392 (2011)

127. Y. Li, W. Wang, X. Qiu, L. Song, M. P. IIIMeyer, G. Paranthaman, Z. Eres, Zhang, and B. Gu, Comparing Cr, and N only doping with (Cr, N)-codoping for enhancing visible light reactivity of TiO_2, *Appl. Catal. B* 110, 148 (2011)

128. M. Chiodi, C. P. Cheney, P. Vilmercati, E. Cavaliere, N. Mannella, H. H. Weitering, and L. Gavioli, Enhanced dopant solubility and visible-light absorption in Cr–N codoped TiO_2 nanoclusters, *J. Phys. Chem. C* 116(1), 311 (2012)

129. J. Jaćimović, R. Gaal, A. Magrez, L. Forró, M. Regmi, and G. Eres, Electrical property measurements of Cr-N codoped TiO_2 epitaxial thin films grown by pulsed laser deposition, *Appl. Phys. Lett.* 102(17), 172108 (2013)

130. Y. Wang, Z. Cheng, S. Tan, X. Shao, B. Wang, and J. Hou, Characterization of Cr–N codoped anatase $TiO_2(001)$ thin films epitaxially grown on $SrTiO_3(001)$ substrate, *Surf. Sci.* 616, 93 (2013)

131. C. P. Cheney, P. Vilmercati, E. W. Martin, M. Chiodi, L. Gavioli, M. Regmi, G. Eres, T. A. Callcott, H. H. Weitering, and N. Mannella, Origins of electronic band gap reduction in Cr/N codoped TiO_2, *Phys. Rev. Lett.* 112(3), 036404 (2014)

132. W. Lu, H. Nguyen, C. Wu, K. Chang, and M. Yoshimura, Modulation of physical and photocatalytic properties of (Cr, N) codoped TiO_2 nanorods using soft solution processing, *J. Appl. Phys.* 115(14), 144305 (2014)

133. Z. Bi, M. P. Paranthaman, B. Guo, R. R. Unocic, C. A. IIIMeyer, X. Bridges, Sun, and S. Dai, High performance Cr, N-codoped mesoporous TiO_2 microspheres for lithium-ion batteries, *J. Mater. Chem. A* 2(6), 1818 (2014)

134. M. Khan, J. Xu, N. Chen, and W. Cao, First principle calculations of the electronic and optical properties of pure and (Mo, N) co-doped anatase TiO_2, *J. Alloys Compd.* 513, 539 (2012)

135. J. Zhang, J. Xi, and Z. Ji, Mo N codoped TiO_2 sheets with dominant {001} facets for enhancing visible-light photocatalytic activity, *J. Mater. Chem.* 22(34), 17700 (2012)

136. M. Li, J. Zhang, and Y. Zhang, Electronic structure and photocatalytic activity of N/Mo doped anatase TiO_2, *Catal. Commun.* 29, 175 (2012)

137. W. Shockley and H. J. Queisser, Detailed balance limit of efficiency of *p–n* junction solar cells, *J. Appl. Phys.* 32(3), 510 (1961)

138. A. Luque and A. Marti, A metallic intermediate band high efficiency solar cell, *Prog. Photovolt. Res. Appl.* 9(2), 73 (2001)

139. H. Katayama-Yoshida, R. Kato, and T. Yamamoto, New valence control and spin control method in GaN and AlN by codoping and transition atom doping, *J. Cryst. Growth* 231(3), 428 (2001)

140. J. Li and J. Kang, Polarization effect on p-type doping efficiency in Mg–Si codoped wurtzite GaN from first-principles calculations, *Phys. Rev. B* 71(3), 035216 (2005)

141. K. H. Ploog and O. Brandt, Doping of group III nitrides, *J. Vac. Sci. Technol. A* 16(3), 1609 (1998)

142. K. S. Kim, C. S. Oh, M. S. Han, C. S. Kim, G. M. Yang, J. W. Yang, C. Hong, C. J. Youn, K. Y. Lim, and H. J. Lee, Co-doping characteristics of Si and Zn with Mg in p-type GaN, *MRS Proceedings* 595, F99W3.84 (1999)

143. T. Kida, Y. Minami, G. Guan, M. Nagano, M. Akiyama, and A. Yoshida, Photocatalytic activity of gallium nitride for producing hydrogen from water under light irradiation, *J. Mater. Sci.* 41(11), 3527 (2006)

144. H. Pan, B. Gu, G. Eres, and Z. Zhang, Ab initio study on noncompensated CrO codoping of GaN for enhanced solar energy conversion, *J. Chem. Phys.* 132(10), 104501 (2010)

145. Z. Xu, Q. Zheng, and G. Su, Charged states and band-gap narrowing in codoped ZnO nanowires for enhanced photoelectrochemical responses: Density functional first-principles calculations, *Phys. Rev. B* 85(7), 075402 (2012)

146. S. Kishimoto, T. Hasegawa, H. Kinto, O. Matsumoto, and S. Iida, Effect and comparison of co-doping of Ag, AgIn, and AgCl in ZnS:N/GaAs layers prepared by vapor-phase epitaxy, *J. Cryst. Growth* 214–215, 556 (2000)

147. T. Yamamoto, S. Kishimoto, and S. Iida, Control of valence states for ZnS by triple-codoping method, *Physica B* 308-310, 916 (2001)

148. M. Muruganandham and Y. Kusumoto, Synthesis of N, C codoped hierarchical porous microsphere ZnS as a visible light-responsive photocatalyst, *J. Phys. Chem. C*113(36), 16144 (2009)

149. H. Sun, X. Zhao, L. Zhang, and W. Fan, Origin of the enhanced visible photocatalytic activity in (N, C)-codoped ZnS studied from density functional theory, *J. Phys. Chem. C* 115(5), 2218 (2011)

150. W. Yin, S. Wei, M. M. Al-Jassim, and Y. Yan, Double-hole-mediated coupling of dopants and its impact on band gap engineering in TiO_2, *Phys. Rev. Lett.* 106(6), 066801 (2011)

151. P. Wang, Z. Liu, F. Lin, G. Zhou, J. Wu, W. Duan, B. Gu, and S. Zhang, Optimizing photoelectrochemical properties of TiO_2 by chemical codoping, *Phys. Rev. B* 82(19), 193103 (2010)

152. J. Li, S. Wei, S. Li, and J. Xia, Design of shallow acceptors in ZnO: First-principles band-structure calculations, *Phys. Rev. B* 74(8), 081201 (2006)

153. X. Zhang, X. Li, T. Chen, C. Zhang, and W. Yu, p-type conduction in wide-gap $Zn_{1-x}Mg_xO$ films grown by ultrasonic spray pyrolysis, *Appl. Phys. Lett.* 87, 2101 (2005)

154. T. Kataoka, Y. Yamazaki, V. Singh, Y. Sakamoto, A. Fujimori, Y. Takeda, T. Ohkochi, S. Fujimori, T. Okane, Y. Saitoh, H. Yamagami, A. Tanaka, M. Kapilashrami, L. Belova, and K. V. Rao, Ferromagnetism in ZnO codoped with Mn and N studied by soft X-ray magnetic circular dichroism, *Appl. Phys. Lett.* 99(13), 132508 (2011)

155. L. Shen, R. Wu, H. Pan, G. Peng, M. Yang, Z. Sha, and Y. Feng, Mechanism of ferromagnetism in nitrogen-doped ZnO: First-principle calculations, *Phys. Rev. B* 78(7), 073306 (2008)

156. H. Jung, C. Song, S. Wang, K. Arai, Y. Wu, Z. Zhu, T. Yao, and H. Katayama-Yoshida, Carrier concentration enhancement of p-type ZnSe and ZnS by codoping with active nitrogen and tellurium by using a d-doping technique, *Appl. Phys. Lett.* 70(9), 1143 (1997)

157. M. Ni, M. K. Leung, D. Y. Leung, and K. Sumathy, A review and recent developments in photocatalytic water-splitting using TiO_2 for hydrogen production, *Renew. Sustain. Energy Rev.* 11(3), 401 (2007)

158. M. Sathish, B. Viswanathan, R. Viswanath, and C. S. Gopinath, Synthesis, characterization, electronic structure, and photocatalytic activity of nitrogen-doped TiO_2 nanocatalyst, *Chem. Mater.* 17(25), 6349 (2005)

159. H. Sun, Y. Bai, Y. Cheng, W. Jin, and N. Xu, Preparation and characterization of visible-light-driven carbon-sulfur-codoped TiO_2 photocatalysts, *Ind. Eng. Chem. Res.* 45(14), 4971 (2006)

160. L. Jia, C. Wu, Y. Li, S. Han, Z. Li, B. Chi, J. Pu, and L. Jian, Enhanced visible-light photocatalytic activity of anatase TiO_2 through N and S codoping, *Appl. Phys. Lett.* 98(21), 211903 (2011)

161. D. B. Hamal and K. J. Klabunde, Valence state and catalytic role of cobalt ions in cobalt TiO_2 nanoparticle photocatalysts for acetaldehyde degradation under visible light, *J. Phys. Chem. C* 115(35), 17359 (2011)

162. A. N. Mangham, N. Govind, M. E. Bowden, V. Shutthanandan, A. G. Joly, M. A. Henderson, and S. A. Chambers, Photochemical properties, composition, and structure in molecular beam epitaxy grown Fe "doped" and (Fe, N) codoped rutile TiO_2(110), *J. Phys. Chem. C* 115(31), 15416 (2011)

163. C. Park, S. Zhang, and S. Wei, Origin of p-type doping difficulty in ZnO: The impurity perspective, *Phys. Rev. B* 66(7), 073202 (2002)

164. K. R. Kittilstved, N. S. Norberg, and D. R. Gamelin, Chemical manipulation of high-T_c ferromagnetism in ZnO diluted magnetic semiconductors, *Phys. Rev. Lett.* 94(14), 147209 (2005)

165. K. R. Kittilstved and D. R. Gamelin, Manipulating polar ferromagnetism in transition metal doped ZnO: Why manganese is different from cobalt, *J. Appl. Phys.* 99, 08M112 (2006)

166. L. Zhao, P. Lu, Z. Yu, X. Guo, Y. Shen, H. Ye, G. Yuan, and L. Zhang, The electronic and magnetic properties of (Mn, N)-codoped ZnO from first principles, *J. Appl. Phys.* 108(11), 113924 (2010)

167. K. Wu, S. Gu, K. Tang, J. Ye, S. Zhu, M. Zhou, Y. Huang, M. Xu, R. Zhang, and Y. Zheng, Temperature-dependent magnetization in (Mn, N)-codoped ZnO-based diluted magnetic semiconductors, *J. Magn. Magn. Mater.* 324(8), 1649 (2012)

168. J. Gaines, R. Drenten, K. Haberern, T. Marshall, P. Mensz, and J. Petruzzello, Blue-green injection lasers containing pseudomorphic $Zn_{1-x}Mg_xS_ySe_{1-y}$ cladding layers and operating up to 394 K, *Appl. Phys. Lett.* 62(20), 2462 (1993)

169. P. Mensz, S. Herko, K. Haberern, J. Gaines, and C. Ponzoni, Electrical characterization of p-type ZnSe:N and $Zn_{1-x}Mg_xS_ySe_{1-y}$:N thin films, *Appl. Phys. Lett.* 63(20), 2800 (1993)

170. S. M. Myers, M. Baskes, H. Birnbaum, J. W. Corbett, G. DeLeo, S. Estreicher, E. E. Haller, P. Jena, N. M. Johnson, R. Kirchheim, S. J. Pearton, and M. J. Stavola, Hydrogen interactions with defects in crystalline solids, *Rev. Mod. Phys.* 64(2), 559 (1992)

171. T. Kuech and J. Redwing, Carbon doping in metalorganic vapor phase epitaxy, *J. Cryst. Growth* 145(1–4), 382 (1994)

172. M. McCluskey, N. Johnson, C. G. Van de Walle, D. P. Bour, M. Kneissl, and W. Walukiewicz, Metastability of oxygen donors in AlGaN, *Phys. Rev. Lett.* 80(18), 4008 (1998)

173. J. I. Pankove and N. M. Johnson (Eds.), Hydrogen in Semiconductors, Hydrogen in SiliconVolume 34 (1991)

174. C. G. Van de Walle and J. Neugebauer, Hydrogen in semiconductors, *Annu. Rev. Mater. Res.* 36(1), 179 (2006)

175. S. Nakamura, Nobel Lecture: Background story of the invention of efficient blue InGaN light emitting diodes, *Rev. Mod. Phys.* 87(4), 1139 (2015)

176. H. Amano, M. Kito, K. Hiramatsu, and I. Akasaki, P-type conduction in Mg-doped GaN treated with low-energy electron beam irradiation (LEEBI), *Jpn. J. Appl. Phys.* 28, L2112 (1989)

177. S. Nakamura, N. Iwasa, M. Senoh, and T. Mukai, Hole compensation mechanism of p-type GaN films, *Jpn. J. Appl. Phys.* 31, 1258 (1992)

178. A. Marinopoulos, Incorporation and migration of hydrogen in yttria-stabilized cubic zirconia: Insights from semilocal and hybrid-functional calculations, *Phys. Rev. B* 86(15), 155144 (2012)

179. S. K. Estreicher, Hydrogen-related defects in crystalline semiconductors: A theorist's perspective, *Mater. Sci. Eng. Rep.* 14(7–8), 319 (1995)

180. M. Stutzmann and J. Chevallier (Eds.), Hydrogen in semiconductors: Bulk and surface properties, *Physica B* 170, 1 (1991)

181. S. J. Pearton, J. W. Corbett, and M. Stavola, Hydrogen in crystalline semiconductors, *Appl. Phys. A* 43(3), 153 (1987)

182. A. J. Morris, C. J. Pickard, and R. Needs, Hydrogen/silicon complexes in silicon from computational searches, *Phys. Rev. B* 78(18), 184102 (2008)

183. A. J. Morris, C. J. Pickard, and R. Needs, Hydrogen/nitrogen/oxygen defect complexes in silicon from computational searches, *Phys. Rev. B* 80(14), 144112 (2009)

184. A. Peles, A. Janotti, and C. Van de Walle, Electrical activity of hydrogen impurities in GaSb: First-principles calculations, *Phys. Rev. B* 78(3), 035204 (2008)

185. V. Darakchieva, K. Lorenz, N. Barradas, E. Alves, B. Monemar, M. Schubert, N. Franco, C. Hsiao, L. Chen, W. Schaff, L. W. Tu, T. Yamaguchi, and Y. Nanishi, Hydrogen in InN: A ubiquitous phenomenon in molecular beam epitaxy grown material, *Appl. Phys. Lett.* 96(8), 081907 (2010)

186. D. Dagnelund, X. Wang, C. Tu, A. Polimeni, M. Capizzi, W. Chen, and I. Buyanova, Effect of post-growth hydrogen treatment on defects in GaNP, *Appl. Phys. Lett.* 98(14), 141920 (2011)

187. D. Dagnelund, I. Vorona, G. Nosenko, X. Wang, C. Tu, H. Yonezu, A. Polimeni, M. Capizzi, W. Chen, and I. Buyanova, Effects of hydrogenation on non-radiative defects in GaNP and GaNAs alloys: An optically detected magnetic resonance study, *J. Appl. Phys.* 111(2), 023501 (2012)

188. N. Balakrishnan, G. Pettinari, O. Makarovsky, L. Turyanska, M. Fay, M. De Luca, A. Polimeni, M. Capizzi, F. Martelli, S. Rubini, and A. Patanè, Band-gap profiling by laser writing of hydrogen-containing III-N-Vs, *Phys. Rev. B* 86(15), 155307 (2012)

189. M. Feneberg, N. T. Son, and A. Kakanakova-Georgieva, Exciton luminescence in AlN triggered by hydrogen and thermal annealing, *Appl. Phys. Lett.* 106(24), 242101 (2015)

190. M. Choi, A. Janotti, and C. G. Van de Walle, Hydrogen passivation of impurities in Al_2O_3, *ACS Appl. Mater. Interfaces* 6(6), 4149 (2014)

191. R. Vidya, P. Ravindran, and H. Fjellvåg, Understanding H-defect complexes in ZnO, arXiv: 1309. 5217 (2013)

192. X. Li, B. Keyes, S. Asher, S. Zhang, S. Wei, T. J. Coutts, S. Limpijumnong, and C. G. Van de Walle, Hydrogen passivation effect in nitrogen-doped ZnO thin films, *Appl. Phys. Lett.* 86(12), 122107 (2005)

193. X. Li, S. E. Asher, S. Limpijumnong, B. M. Keyes, C. L. Perkins, T. M. Barnes, H. R. Moutinho, J. M. Luther, S. Zhang, S. Wei, and T. J. Coutts, Impurity effects in ZnO and nitrogen-doped ZnO thin films fabricated by MOCVD, *J. Cryst. Growth* 287(1), 94 (2006)

194. S. Lin, H. He, Y. Lu, and Z. Ye, Mechanism of Na-doped p-type ZnO films: Suppressing Na interstitials by codoping with H and Na of appropriate concentrations, *J. Appl. Phys.* 106(9), 093508 (2009)

195. F. Filippone, G. Mattioli, P. Alippi, and A. Amore Bonapasta, Properties of hydrogen and hydrogen–vacancy complexes in the rutile phase of titanium dioxide, *Phys. Rev. B* 80(24), 245203 (2009)

196. H. Pan, Y. Zhang, V. B. Shenoy, and H. Gao, Effects of H-, N-, and (H, N)-doping on the photocatalytic activity of TiO_2, *J. Phys. Chem. C* 115(24), 12224 (2011)

197. C. Park and D. Chadi, Hydrogen-mediated spin-spin interaction in ZnCoO, *Phys. Rev. Lett.* 94(12), 127204 (2005)

198. M. Assadi, Y. Zhang, and S. Li, Hydrogen multicenter bond mediated magnetism in Co doped ZnO, *J. Phys.: Condens. Matter* 22(15), 156001 (2010)

199. K. Wu, S. Gu, K. Tang, J. Ye, S. Zhu, M. Zhou, Y. Huang, M. Xu, R. Zhang, and Y. Zheng, Hydrogen diffusion behavior and its effect on magnetic properties in (Mn, N)-codoped ZnO, *Physica B* 454, 115 (2014)

200. S. Nehra and M. Singh, Role of hydrogen in CdTe–Mn thin film bilayer structure, *J. Alloys Compd.* 488(1), 356 (2009)

201. S. Nehra, M. Jangid, S. Srivastava, A. Kumar, B. Tripathi, M. Singh, and Y. Vijay, Role of hydrogen in electrical and structural characteristics of bilayer CdTe/Mn diluted magnetic semiconductor thin films, *Int. J. Hydrogen Energy* 34(17), 7306 (2009)

202. S. Nehra and M. Singh, Effect of vacuum annealing and hydrogenation on ZnSe/Mn multilayer diluted magnetic semiconductor thin films, *Vacuum* 85(7), 719 (2011)

203. R. Nazarov, T. Hickel, and J. Neugebauer, First-principles study of the thermodynamics of hydrogen-vacancy interaction in fcc iron, *Phys. Rev. B* 82(22), 224104 (2010)

204. Y. Tateyama and T. Ohno, Stability and clusterization of hydrogen-vacancy complexes in α-Fe: An *ab initio* study, *Phys. Rev. B* 67(17), 174105 (2003)

205. G. Lu and E. Kaxiras, Hydrogen embrittlement of aluminum: the crucial role of vacancies, *Phys. Rev. Lett.* 94(15), 155501 (2005)

206. O. Y. Vekilova, D. Bazhanov, S. Simak, and I. Abrikosov, First-principles study of vacancy-hydrogen interaction in Pd, *Phys. Rev. B* 80(2), 024101 (2009)

207. W. Theis, K. Bajaj, C. Litton, and W. Spitzer, Direct evidence for the site of substitutional carbon impurity in GaAs, *Appl. Phys. Lett.* 41(1), 70 (1982)

208. J. Geisz, D. Friedman, J. Olson, S. R. Kurtz, and B. Keyes, Photocurrent of 1eV GaInNAs lattice-matched to GaAs, *J. Cryst. Growth* 195(1–4), 401 (1998)

209. C. Seager, A. Wright, J. Yu, and W. Götz, Role of carbon in GaN, *J. Appl. Phys.* 92(11), 6553 (2002)

210. M. McCluskey, E. Haller, and P. Becla, Carbon acceptors and carbon-hydrogen complexes in AlSb, *Phys. Rev. B* 65(4), 045201 (2001)

211. M. Strassburg, J. Senawiratne, N. Dietz, U. Haboeck, A. Hoffmann, V. Noveski, R. Dalmau, R. Schlesser, and Z. Sitar, The growth and optical properties of large, high-quality AlN single crystals, *J. Appl. Phys.* 96(10), 5870 (2004)

212. J. Lyons, A. Janotti, and C. Van de Walle, Carbon impurities and the yellow luminescence in GaN, *Appl. Phys. Lett.* 97(15), 152108 (2010)

213. J. Lyons, A. Janotti, and C. Van de Walle, Effects of carbon on the electrical and optical properties of InN, GaN, and AlN, *Phys. Rev. B* 89(3), 035204 (2014)

214. S. G. Christenson, W. Xie, Y. Sun, and S. Zhang, Carbon as a source for yellow luminescence in GaN: Isolated CN defect or its complexes, *J. Appl. Phys.* 118(13), 135708 (2015)

215. K. Tang, S. Gu, S. Zhu, J. Liu, H. Chen, J. Ye, R. Zhang, and Y. Zheng, Suppression of compensation from nitrogen and carbon related defects for p-type N-doped ZnO, *Appl. Phys. Lett.* 95(19), 192106 (2009)

216. A. Marzouki, A. Lusson, F. Jomard, A. Sayari, P. Galtier, M. Oueslati, and V. Sallet, SIMS and Raman characterizations of ZnO:N thin films grown by MOCVD, *J. Cryst. Growth* 312(21), 3063 (2010)

217. J. Liu, S. Gu, S. Zhu, K. Tang, X. Liu, H. Chen, and Y. Zheng, The influences of O/Zn ratio and growth temperature on carbon impurity incorporation in ZnO grown by metal-organic chemical vapor deposition, *J. Cryst. Growth* 312(19), 2710 (2010)

218. A. Marzouki, A. Sayari, F. Jomard, V. Sallet, A. Lusson, and M. Oueslati, Carrier gas and VI/II ratio effects on carbon clusters incorporation into ZnO films grown by MOCVD, *Mater. Sci. Semicond. Process.* 16(3), 1022 (2013)

219. H. Mao, S. Gu, J. Ye, K. Tang, R. Gu, S. Zhu, S. Huang, Z. Yao, and Y. Zheng, Comparative study of the effect of H_2 addition on ZnO films grown by different zinc and oxygen precursors, *J. Mater. Res.* 30(07), 935 (2015)

220. K. Tang, S. Gu, S. Zhu, W. Liu, J. Ye, J. Zhu, R. Zhang, Y. Zheng, and X. Sun, Carbon clusters in N-doped ZnO by metal-organic chemical vapor deposition, *Appl. Phys. Lett.* 93(13), 132107 (2008)

221. H. Chen, S. Gu, W. Liu, S. Zhu, and Y. Zheng, Influence of unintentional doped carbon on growth and properties of N-doped ZnO films, *J. Appl. Phys.* 104(11), 113511 (2008)

222. N. Nickel, F. Friedrich, J. Rommeluère, and P. Galtier, Vibrational spectroscopy of undoped and nitrogen-doped ZnO grown by metalorganic chemical vapor deposition, *Appl. Phys. Lett.* 87(21), 211905 (2005)

223. X. Li, S. E. Asher, S. Limpijumnong, S. Zhang, S. Wei, T. M. Barnes, T. J. Coutts, and R. Noufi, Unintentional doping and compensation effects of carbon in metal-organic chemical-vapor deposition fabricated ZnO thin films, *J. Vac. Sci. Technol. A* 24(4), 1213 (2006)

224. L. L. Kerr, X. Li, M. Canepa, and A. J. Sommer, Raman analysis of nitrogen doped ZnO, *Thin Solid Films* 515(13), 5282 (2007)

225. S. Limpijumnong, X. Li, S. Wei, and S. Zhang, Substitutional diatomic molecules NO, NC, CO, N_2, and O_2: Their vibrational frequencies and effects on p doping of ZnO, *Appl. Phys. Lett.* 86(21), 211910 (2005)

226. K. Wu, S. Gu, K. Tang, S. Zhu, J. Ye, R. Zhang, and Y. Zheng, Influences of unintentionally doped carbon on magnetic properties in Mn–N co-doped ZnO, *Thin Solid Films* 519(8), 2499 (2011)

227. S. Tan, X. Sun, Z. Yu, P. Wu, G. Lo, and D. Kwong, p-type conduction in unintentional carbon-doped ZnO thin films, *Appl. Phys. Lett.* 91(7), 072101 (2007)

228. M. Yoshikawa, S. Ueda, K. Maruyama, and H. Takigawa, The behavior of oxygen in HgCdTe, *J. Vac. Sci. Technol. A* 3(1), 153 (1985)

229. M. Toth, K. Fleischer, and M. Phillips, Direct experimental evidence for the role of oxygen in the luminescent properties of GaN, *Phys. Rev. B* 59(3), 1575 (1999)

230. H. W. Jang, J. M. Baik, M. Lee, H. Shin, and J. Lee, Incorporation of oxygen donors in AlGaN, *J. Electrochem. Soc.* 151(8), G536 (2004)

231. S. Das Bakshi, J. Sumner, M. J. Kappers, and R. A. Oliver, The influence of coalescence time on unintentional doping in GaN/sapphire, *J. Cryst. Growth* 311(2), 232 (2009)

232. B. Mitchell, D. Timmerman, Z. Wiaxing, J. Takatsu, M. Matsuda, K. Lorenz, E. Alves, A. Koizumi, Y. Fujiwara, and V. Dierolf, The role of oxygen on the nature and stability of Eu centers in Eu doped gallium nitride, APS March Meeting 2015, abstract #F14.007

233. C. King, R. Johnson, T. Chiu, J. Sung, and M. Morris, Suppression of arsenic autodoping with rapid thermal epitaxy for low power bipolar complementary metal oxide semiconductor, *J. Electrochem. Soc.* 142(7), 2430 (1995)

234. Van de Wallea, G. Chris, and J. Neugebauer, Arsenic impurities in GaN, *Appl. Phys. Lett.* 8, 76 (2000)

235. H. Kim, F. J. Fälth, and T. G. Andersson, Unintentional incorporation of B, As, and O impurities in GaN grown by molecular beam epitaxy, *J. Electron. Mater.* 30(10), 1343 (2001)

236. R. Vidya, P. Ravindran, H. Fjellvåg, B. Svensson, E. Monakhov, M. Ganchenkova, and R. Nieminen, Energetics of intrinsic defects and their complexes in ZnO investigated by density functional calculations, *Phys. Rev. B* 83(4), 045206 (2011)

237. Y. Lu, S. Russo, and Y. Feng, Effect of nitrogen and intrinsic defect complexes on conversion efficiency of ZnO for hydrogen generation from water, *Phys. Chem. Chem. Phys.* 13(35), 15973 (2011)

238. S. Chen, J. Yang, X. Gong, A. Walsh, and S. Wei, Intrinsic point defects and complexes in the quaternary kesterite semiconductor Cu_2ZnSnS_4, *Phys. Rev. B* 81(24), 245204 (2010)

239. M. Copel, M. Reuter, E. Kaxiras, and R. Tromp, Surfactants in epitaxial growth, *Phys. Rev. Lett.* 63(6), 632 (1989)

240. H. Van der Vegt, H. Van Pinxteren, M. Lohmeier, E. Vlieg, and J. Thornton, Surfactant-induced layer-by-layer growth of Ag on Ag(111), *Phys. Rev. Lett.* 68(22), 3335 (1992)

241. G. Rosenfeld, R. Servaty, C. Teichert, B. Poelsema, and G. Comsa, Layer-by-layer growth of Ag on Ag(111) induced by enhanced nucleation: A model study for surfactant-mediated growth, *Phys. Rev. Lett.* 71(6), 895 (1993)

242. J. Meyer, J. Vrijmoeth, H. Van der Vegt, E. Vlieg, and R. Behm, Importance of the additional step-edge barrier in determining film morphology during epitaxial growth, *Phys. Rev. B* 51(20), 14790 (1995)

243. B. Voigtländer, A. Zinner, T. Weber, and H. P. Bonzel, Modification of growth kinetics in surfactant-mediated epitaxy, *Phys. Rev. B* 51(12), 7583 (1995)

244. S. Tanaka, S. Iwai, and Y. Aoyagi, Self-assembling GaN quantum dots on $Al_xGa_{1-x}N$ surfaces using a surfactant, *Appl. Phys. Lett.* 69(26), 4096 (1996)

245. E. Rudkevich, F. Liu, D. Savage, T. Kuech, L. McCaughan, and M. Lagally, Hydrogen induced Si surface segregation on Ge-covered Si(001), *Phys. Rev. Lett.* 81(16), 3467 (1998)

246. M. Pillai, S. Kim, S. Ho, and S. Barnett, Growth of $In_xGa_{1-x}As$/GaAs heterostructures using Bi as a surfactant, *J. Vac. Sci. Technol. B* 18(3), 1232 (2000)

247. C. Fetzer, R. Lee, J. Shurtleff, G. Stringfellow, S. Lee, and T. Seong, The use of a surfactant (Sb) to induce triple period ordering in GaInP, *Appl. Phys. Lett.* 76(11), 1440 (2000)

248. A. Howard and G. Stringfellow, Effects of low surfactant Sb coverage on Zn and C incorporation in GaP, *J. Appl. Phys.* 102(7), 074920 (2007)

249. J. Zhu, F. Liu, and G. Stringfellow, Dual-surfactant effect to enhance p-type doping in III-V semiconductor thin films, *Phys. Rev. Lett.* 101(19), 196103 (2008)

250. A. Howard and G. Stringfellow, Effects of dimethylhydrazine on Zn, C, and H doping of GaP, *J. Cryst. Growth* 310(11), 2702 (2008)

251. L. Zhang, Y. Yan, and S. Wei, Enhancing dopant solubility via epitaxial surfactant growth, *Phys. Rev. B* 80(7), 073305 (2009)

252. J. Zhu, F. Liu, and G. Stringfellow, Enhanced cation-substituted p-type doping in GaP from dual surfactant effects, *J. Cryst. Growth* 312(2), 174 (2010)

253. A. Howard, D. Chapman, and G. Stringfellow, Effects of surfactants Sb and Bi on the incorporation of zinc and carbon in III/V materials grown by organometallic vapor-phase epitaxy, *J. Appl. Phys.* 100(4), 044904 (2006)

254. T. Sato, M. Mitsuhara, R. Iga, S. Kanazawa, and Y. Inoue, Influence of Sb surfactant on carrier concentration in heavily Zn-doped InGaAs grown by metalorganic vapor phase epitaxy, *J. Cryst. Growth* 315(1), 64 (2011)

255. J. Zhu and S. Wei, Overcoming doping bottleneck by using surfactant and strain, *Front. Mater. Sci.* 5(4), 335 (2011)

256. V. Wagener, M. Wagener, and J. Botha, Electrical characteristics of cadmium doped InAs grown by metalorganic vapor phase epitaxy, *J. Appl. Phys.* 111(2), 023707 (2012)

257. S. Kahwaji, R. Gordon, E. Crozier, S. Roorda, M. Robertson, J. Zhu, and T. Monchesky, Surfactant-mediated growth of ferromagnetic Mn d-doped Si, *Phys. Rev. B* 88(17), 174419 (2013)

258. J. Zhu, F. Liu, G. Stringfellow, and S. Wei, Strain-enhanced doping in semiconductors: Effects of dopant size and charge state, *Phys. Rev. Lett.* 105(19), 195503 (2010)

259. J. Zhu and S. Wei, Tuning doping site and type by strain: Enhanced p-type doping in Li doped ZnO, *Solid State Commun.* 151(20), 1437 (2011)

260. B. Deng, Y. Zhang, S. Zhang, Y. Wang, K. He, and J. Zhu, Realization of stable ferromagnetic order in topological insulator: Co-doping enhanced magnetism in 4f transition metal doped Bi_2Se_3, arXiv: 1511.08646 (2015)

261. J. L. Merrell, F. Liu, and G. B. Stringfellow, Effect of surfactant Sb on In incorporation and thin film morphology of InGaN layers grown by organometallic vapor phase epitaxy, *J. Cryst. Growth* 375, 90 (2013)

262. Y. Zhang and J. Zhu, Surfactant antimony enhanced indium incorporation on InGaN (0001) surface: A DFT study, *J. Cryst. Growth* 438, 43 (2016)